Mouse Models for Allergic Asthma: Effect of Acute Allergen Challenge on Pulmonary Function and Airway Inflammation in Caveolin-1 Knockout Mice

Sarah Martin
Supervisors: Dr. Andrew Halayko and Dr. Ganesh Srinivasan

A thesis submitted in partial fulfillment of the Honours Thesis (05.4111/6) Course
Department of Biology
The University of Winnipeg
2006

Abstract

Caveolin-1 is a scaffolding protein which induces cave-like plasma membrane invaginations, known as caveolae. Caveolae are abundant in most lung cells and regulate receptor activation of intracellular signaling pathways. Airway epithelial cells and airway smooth muscle contribute significantly to local inflammation in response to inhaled allergic and non-allergic compounds via caveolae-associated receptors. G-protein coupled receptors, important for airway smooth muscle contraction, are also associated with and regulated by caveolae. These factors suggest that caveolin-1 could potentially modulate airway smooth muscle contraction, as well as inflammatory responses that are important in the pathogenesis of asthma. We hypothesized that caveolin-1 expression is a determinant both of airway structure and function, and of inflammatory responses to inhaled allergic proteins. Genetic control strain (B6129SF2/J) and caveolin-1 knockout mice were sensitized twice with intraperitoneal injections of ovalbumin and challenged twice intranasally with ovalbumin. Lung function was measured by whole body plethysmography and expressed as enhanced pause (Penh). Baseline Penh values were 50% lower ($P<0.05$) in caveolin-1 knockout mice for methacholine exposures up to 50mg/ml. Differential cell counts from bronchoalveolar lavage fluid revealed that sensitization and challenge decreased macrophages and increased eosinophils; however, this inflammation occurred to a lesser extent in caveolin-1 knockout mice. Increased alveolar septal thickening and airway epithelial hyperplasia was seen in caveolin-1 knockout mice. Trichrome staining showed prominent airway smooth muscle and excessive extracellular matrix around airways and blood vessels. Collectively, the data suggests that caveolin-1 modulates airway function and orchestrates local allergic inflammation. Thus, further studies to dissect its role in asthma pathogenesis are highly warranted.

Acknowledgements

I would like to express my gratitude to my wonderful supervisors, Dr. Andrew Halayko, and Dr. Ganesh Srinivasan. Their knowledge and support were crucial in the completion of this project. I would especially like to thank Sujata Basu for all of her help in the lab, for teaching me the technical skills required to complete this research, and for her support throughout. I would also like to acknowledge all the members of the Halayko lab: Reinoud, Thai, Karol, Gerald, Mark, and Karen for their assistance, sense of humour and advice in the lab. The Biology of Breathing Research Theme members were always willing to answer my questions and I wish to express my gratitude to them for providing an interactive research environment. I would also like to thank my committee member, Dr. Wiegand, for stimulating my interest in medical physiology. Finally, I would like to thank the Manitoba Institute of Child Health at the John Buhler Research Centre for the use of their facility and equipment.

Table of Contents

Page

Abstract....ii

Acknowledgements....iii

Table of Contents....iv

List of Tables....vi

List of Figures....vii

List of Appendices....viii

1. Introduction....1

1.1 Asthma....1

1.2 Mouse Models of Asthma....2

1.3 Whole Body Plethysmography....4

1.4 Lipid Rafts....6

1.5 Caveolae and Caveolin-1....6

1.6 Caveolin-1 knockout mice....9

1.7 Hypothesis....11

2. Materials and Methods....12

2.1 Allergen Sensitization and Challenge Protocol....12

2.2 Whole Body Plethysmography....13

2.3 Bronchoalveolar Lavage and Cell Differentials....15

2.3.1 Bronchoalveolar Lavage....16

2.3.2 Cell Differentials....16

2.4 Histology....16

2.4.1 Deparaffinization and Rehydration....17

2.4.2 Hematoxylin and Eosin Stain....17

2.4.3 Masson's Trichrome Stain....18

2.4.4 Rehydration and Clearing....19

2.4.5 Image Analysis....19

2.5 Statistical Analysis....19

3. Results....20

3.1 BALB/c mice experiments....20

3.1.1 Lung Function....20

3.1.2 Bronchoalveolar lavage fluid (BALF) cell differentials....22

3.2 Caveolin-1 knockout mice experiments....24
3.2.1 Lung Function....24
3.2.2 Bronchoalveolar lavage fluid (BALF) cell differentials....28
3.2.3 Histology....31
4. Discussion....34
4.1 Conclusion....39
5. References....41
6. Appendix....46

List of Tables

Page

Table 1 Procedure for Processing Lung Tissue.....17

Table 2 Procedures for Deparaffinization and Rehydration.....17

Table 3 Procedures for Dehydration and Clearing.....19

List of Figures

Page

Figure 1 Changes in box pressure waveform after methacholine exposure.....5

Figure 2 Schematic of a caveolae and its associations with G protein.....8
coupled and growth factor receptors

Figure 3 Allergen sensitization and challenge protocol.....13

Figure 4 Schematic of a box pressure wave explaining the calculation of.....14
enhanced pause (Penh)

Figure 5 Buxco whole body plethysmograph system set up.....15

Figure 6 Penh response in allergen and saline sensitized and challenged.....21
BALB/c mice

Figure 7 Effect of allergen sensitization and challenge on maximum Penh.....22
response in BALB/c mice

Figure 8 Effect of allergen sensitization and challenge on BALB/c.....24
bronchoalveolar lavage fluid (BALF) cell differentials

Figure 9 Penh response in caveolin-1 knockout (Cav-1 KO) and 27
genetic control(B6129SF2/J) mice before and after OVA
sensitization and challenge

Figure 10 Comparison of maximum Penh response after allergen sensitization.....28
and challenge in caveolin-1 knockout (Cav-1 KO) and B6129SF2/J mice

Figure 11 Effect of OVA sensitization and challenge on caveolin-1 knockout.....30
(Cav-1 KO) and B6129SF2/J bronchoalveolar lavage fluid (BALF) cell
differentials

Figure 12 Hematoxylin and Eosin (H&E) staining of lung sections from.....31
a naïve caveolin-1 knockout animal (Cav-1 KO) (A) (C) and a naïve
genetic control animal (B6129SF2/J) (B) (D)

Figure 13 Masson's Trichrome staining of lung tissue sections from a.....32
naïve caveolin-1 knockout mouse (Cav-1 KO) (A) and a naïve genetic
control animal (B6129SF2/J) (B)

Figure 14 Masson's Trichrome staining of lung parenchyma from a naïve.....33
caveolin-1 knockout mouse (Cav-1 KO) (A) and a naïve genetic
control mouse (B6129SF2/J) (B)

Figure 15 Preparation of methacholine solutions by serial dilution.....46

List of Appendices

Page

6.1 Recipes.....46
6.1.1 Methacholine Preparation.....46
6.1.2 Wiegert's Iron Hematoxylin Preparation.....46
6.1.3 Phosphotungstic/Phosphomolybdic acid solution.....46

1. Introduction

1.1 Asthma

Asthma is a significant cause of morbidity worldwide. Currently, 10% of Canadian children and 5% of adults have asthma, but a significant trend for increasing prevalence is developing (The National Asthma Control Task Force 2000). World wide rates are on average increasing by 50% every decade (The National Asthma Control Task Force 2000). The disease continues to be the major cause of hospitalization and school absenteeism among children, and accounts for approximately 600 million dollars each year in direct costs (The National Asthma Control Task Force 2000). Many current asthma therapies relieve symptoms, but do not prevent the progression of the disease. As a result, disease morbidity increases in individual patients with disease duration. It therefore becomes important to understand the cellular mechanisms which contribute to asthma pathogenesis.

Asthmatic airways are often referred to as being "twitchy" because they overreact to stimuli, such as allergens, which are harmless to others. During an asthma attack, the smooth muscle surrounding the airways contracts (The National Asthma Control Task Force 2000). This narrows the lumen of the airway, thus limiting airflow and making breathing difficult. This reaction is known as bronchoconstriction and current therapies focus on controlling and reversing these asthma attacks.

Asthma is diagnosed by measuring the breathing response in patients after inhalation of agents that cause reversible contraction of airway smooth muscle, known as bronchoconstrictors (eg. methacholine). The test mimics the effect of an asthma attack. Since asthmatics have hypersensitive and hyperreactive airway smooth muscle, their breathing will be more difficult, and will be affected by lower concentrations of inhaled bronchoconstrictors (Cockcroft 1985). This response is known as airway hyperresponsiveness and is a characteristic feature of asthma (Cockcroft 1985). Using clinical guidelines, airway

hyperresponsiveness is diagnosed when an increase in airway resistance of more than 20% occurs in response to less than 8mg/ml of inhaled methacholine (Boulet *et al.,* 2006).

Atopic or allergic asthma is common and develops from repeated exposure to allergens, such as ragweed pollen, dust mite and tree pollen (Epstein 2004). It is an inflammatory disease of the airways and is characterized by increased immunoglobulin E (IgE) serum levels, eosinophilic and neutrophilic lung inflammation, increased mucus secretion, as well as airway hyperresponsiveness (Epstein 2004). Eosinophils are particularly important in asthma because their activation leads to the release of inflammatory mediators which cause tissue damage, bronchoconstriction and contribute to the chronic inflammation in long time asthma sufferers (Whitehead *et al.,* 2003). Though other inflammatory airway diseases such as bronchitis exist, these diseases are distinct from asthma in that cytocellular inflammation is not primarily eosinophilic in nature (Epstein 2004; Whitehead *et al.,* 2003).

With disease progression, and repeated allergen exposure, a progressive remodelling of the airways can occur. This process involves airway smooth muscle hyperplasia and hypertrophy, subepithelial fibrosis and mucus gland and goblet cell hyperplasia (Bai *et al.,* 2005; Redington 2000). Airway remodelling results in the irreversible loss of lung function and contributes to the chronic airway hyperresponsiveness in long-time asthma sufferers (Bai *et al.,* 2005).

1.2 Mouse models of asthma

Epidemiological studies and clinical investigation face constraints that can be overcome using animal models. For example, ethical issues limit the study of allergen sensitization in humans, and testing novel treatments is difficult because of the strict guidelines that need to be met before a drug is accepted for clinical trials. Animal models have been developed and have allowed researchers to expand our understanding of the pathophysiology of asthma through the pre-clinical testing of different protocols not suitable for human trials. The advanced understanding of the mouse immune system and the availability of genetically altered mice have increased the use of mouse models for allergic diseases, such as asthma.

Although mouse models rarely encompass all features of human disease, following sensitization and challenge with allergen, mice develop some of the features of allergic asthma (Epstein 2004). The majority of mouse models utilize a sensitization and challenge technique to induce asthma-like airway inflammation (Epstein 2004). In mice, prior to lung challenge, systemic immunity is achieved through intraperitoneal (*i.p.*) immunization (Epstein 2004). Most allergen sensitization protocols involve two *i.p.* immunizations, in which the second injection increases the number of circulating antigen-specific T cells. These cells are required for the initiation of allergic asthma-like inflammation in mice (Epstein 2004). Antigens are often added to alum ($Al(OH)_3$) for *i.p.* injection to enhance immunity, eosinophilia, and the severity of asthma-like symptoms in mice(Alkan *et al.,* 1996; Epstein 2004; Mojtabavi *et al.,* 2002).

To induce acute asthma-like allergic inflammation in the airways, following sensitization or priming, mice undergo repeated respiratory tract antigen challenges. These challenges are most often accomplished through intranasal, intratracheal or aerosol methods (Epstein 2004). Mice will not develop allergic asthma-like airway inflammation, unless they receive both sensitization through *i.p.* followed by respiratory challenges (Epstein 2004).

The most commonly used antigen in mouse models is ovalbumin (OVA); however, other allergens implicated in human disease, such as cockroach antigens (Kim *et al.,* 2001), ragweed pollen (Cates *et al.,* 2003; Justice *et al.,* 2002) and house dust mite antigens(O'Brien *et al.,* 1996; Yu *et al.,* 1999) are also often used with similar effects. This indicates that the immunity and subsequent disease in mice is an allergen induced phenomenon, but is not allergen-specific.

While conjugating antigen with alum promotes disease induction, several factors act to reduce the severity of the disease in mice. For instance, male mice show less severe allergic asthma-like inflammation following sensitization and challenge, suggesting that gender may

play an influential role (Epstein 2004). As a result, most researchers use female mice for modeling allergic asthma.

1.3 Whole body plethysmography

Unrestrained whole body plethysmography (WBP) is a non-invasive method for measuring lung function in live, unrestrained animals. Several different approaches have been used to measure airway function in mice. The *in vitro* measurement of airway smooth muscle contractility after stimulation with an electric field correlates well with allergic airway sensitization (Hamelmann *et al.,* 1997). However, the influence of mucus production and other changes in the lower airways after sensitization are not reflected with this technique (Hamelmann *et al.,* 1997). The *in vivo* measurement of lung resistance or compliance using small animal ventilators is an accurate method of measuring airway responsiveness (Eum *et al.,* 2005; Wagers *et al.,* 2004). This technique requires anaesthesia and involves ventilating the animals. It is much more technically demanding, more time consuming and only one animal can be studied at a time. Also, the intravenous introduction of bronchoconstrictors required in this method may not reflect the stimulation of airway smooth muscles (Hamelmann *et al.,* 1997).

Whole body plethysmography is advantageous because it allows for repeated and long term measurements of lung function since it is not invasive and is not an experimental endpoint. Also, the inhalation of aerosolized bronchoconstrictors allows for the direct stimulation of airway smooth muscle. WBP does not directly measure airway responsiveness; rather, it provides an index of total lung function that is often chiefly determined by airway responses. Furthermore, measurements of lung function by WBP have been shown to correlate well with airway hyperresponsiveness in BALB/c mice (Adler *et al.,* 2004; Whitehead *et al.,* 2003). Hamelmann *et al.* (1997) compared the results from several techniques used to measure airway responsiveness and concluded WBP is a valid indicator of airway

hyperresponsiveness after allergic sensitization in mice. This has subsequently been confirmed by other researchers (Borchers *et al.,* 2003; Henderson *et al.,* 2002; Khan *et al.,* 2002).

Whole body plethysmography measures changes in lung function through the calculation of a dimensionless parameter, enhanced pause (Penh). Penh measures the changes in inspiration and expiration rate and volume following methacholine exposure; changes in breathing patterns are represented as changes in box pressure waveform (Hamelmann *et al.,* 1997). For example, during methacholine-induced bronchoconstriction, the alteration in the signal is more distinct during expiration than inspiration, which is reflected by an increase in Penh (Figure 1)(Hamelmann *et al.,* 1997). Thus, the difficulty breathing experienced during bronchoconstriction is correlated with an increase in Penh value. See section 2.2 for details.

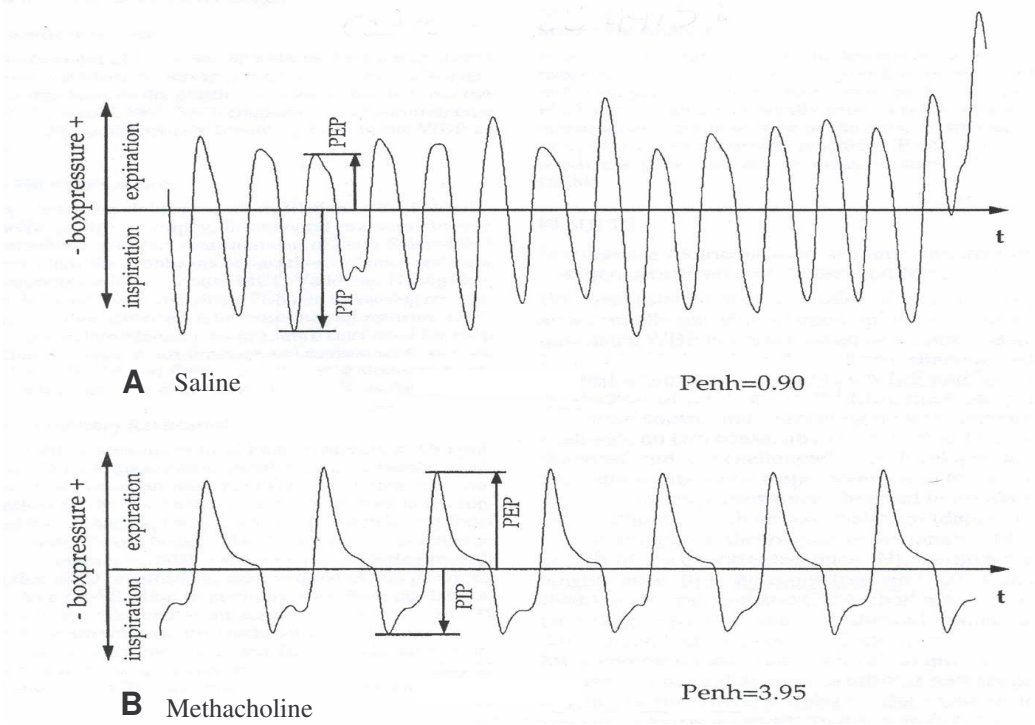

Figure 1: Changes in box pressure waveform after methacholine exposure. Waveform box pressure signal from a normal mouse following exposure to aerosolized saline **(A)** or aerosolized methacholine (50 mg/ml) **(B)**. Peak expiratory pressure (PEP) is the maximum pressure observed during expiration. Peak inspiratory pressure (PIP) is the maximum pressure observed during inspiration. Penh changes with alterations in the signal due to increased time for expiration. The increase in Penh reflects the difficulty breathing experienced during bronchoconstriction.(Hamelmann *et al.,* 1997)

1.4 Lipid Rafts

For many years, the plasma membrane of cells was thought to resemble the fluid mosaic model proposed by Singer and Nicholson (1972). This model implied that all plasma membrane proteins were dispersed uniformly and lipids were loosely packed, allowing for rapid lateral diffusion. This viewpoint has been altered with the discovery of plasma membrane components that are organized into discrete regions or domains, specialized for specific cell functions. Several researchers have described regions of the plasma membrane called "lipid rafts" which are rich in cholesterol and sphingolipids, making them more ordered and less fluid-like compared to the surrounding plasma membrane (Galbiati *et al.,* 2001). These characteristics result in detergent insolubility and a light, buoyant density which allows for their isolation from other membrane fractions (Simons *et al.,* 1997).

Lipid rafts organize the plasma membrane into microdomains which act as platforms for the conduction of a variety of cellular functions, including vesicular trafficking and signal transduction (Simons *et al.,* 1997). While classic lipid rafts lack structural proteins, some liquid ordered domains, such as caveolae, may be enriched in structural proteins which drastically change both the morphology and function of the lipid raft (Galbiati *et al.,* 2001).

1.5 Caveolins and Caveolae

Caveolae are vesicular organelles of the plasma membrane measuring 50 – 100 nm in diameter (Figure 2) (Hnasko *et al.,* 2003). They were discovered by Palade and received their name in 1955 after being described as structures which resembled "little caves" by Yamada (Bergdahl *et al.,* 2004; Hnasko *et al.,* 2003; Yamada 1955). These flask-like invaginations are considered to be a subset of lipid rafts, due to their distinct lipid composition. Rich in cholesterol, sphingomyelin and glycosphingolipids, caveolae are abundant in most cells including fibroblasts, adipocytes, endothelial and epithelial cells, as well as smooth and striated muscle, suggesting they play an important role in cell physiology (Smart *et al.,* 1999; Williams *et al.,* 2004). These structures have many diverse functions including endocytosis, membrane

trafficking, regulation of cholesterol homeostasis, and they are associated with many signal transduction pathways (Hnasko *et al.,* 2003; Razani *et al.,* 2001a).

Caveolae are characterized by the presence of scaffolding proteins, called caveolins, which distinguish these liquid ordered domains from lipid rafts (Li *et al.,* 2005). To date, three caveolins have been identified. Caveolin-1 and caveolin-2 are co-expressed in many tissues while caveolin-3 expression is skeletal muscle specific (Smart *et al.,* 1999). The caveolin gene family is conserved both structurally and functionally from *Caenorhabditis elegans* (worms) to humans, supporting the idea that these proteins are essential for normal cellular function (Galbiati *et al.,* 2001).

Of the caveolins, caveolin-1 is the most extensively characterized. It is a 22-24 kDa intracellular cell membrane associated protein which binds cholesterol with high affinity, and is essential for the formation of caveolae (Galbiati *et al.,* 2001; Hnasko *et al.,* 2003; Murata *et al.,* 1995). The 20-residue hydrophobic scaffolding domain of caveolin-1 interacts with a variety of signaling proteins including H-Ras, c-Src, insulin receptor, endothelial nitric oxide synthase (eNOS), and Gα subtypes, resulting in associations with many signal transduction pathways (Hnasko *et al.,* 2003)(Figure 2). The interaction of the caveolin-1 scaffolding domain with caveolin-binding domains in these proteins, results in the inhibition of downstream signaling (Figure 2)(Williams *et al.,* 2004). Following an appropriate stimulus, caveolin-1 and the signaling molecule disassociate, allowing for the propagation of downstream signaling. One of the best documented examples of caveolae involvement in the cardiovascular system is the regulation of eNOS. It is inactivated when bound to caveolin-1, but when intracellular calcium levels increase, eNOS is displaced from caveolin-1. This displacement results in the production of nitric oxide (NO), which promotes vasodilation (Garcia-Cardena *et al.,* 1996; Ghosh *et al.,* 1998; Michel *et al.,* 1997a; Michel *et al.,* 1997b).

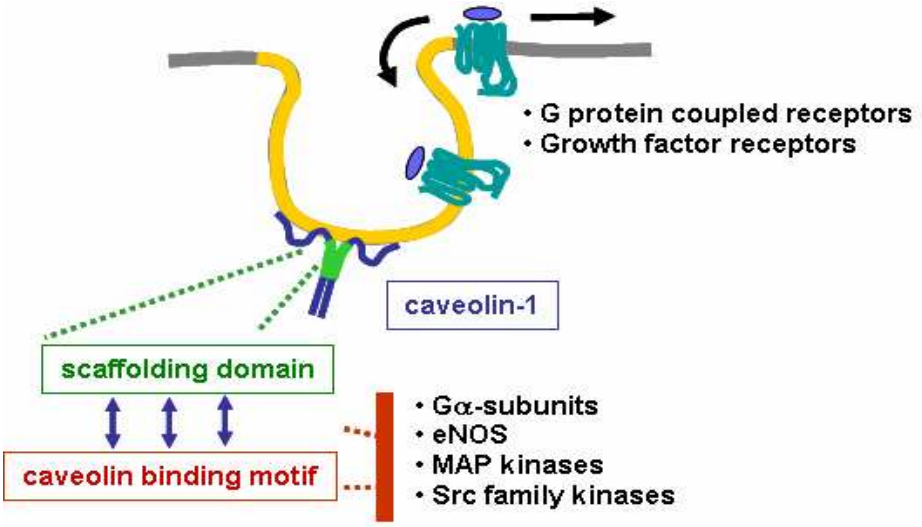

Figure 2: Schematic of a caveolae and its associations with G protein coupled and growth factor receptors. Caveolae are plasma membrane (grey) invaginations which are associated with G protein coupled receptors and growth factor receptors (teal). These receptors are able to move in and out of the caveolae allowing for activation of other signaling molecules colocalized in caveolae (not shown). Caveolin-1 (blue) is a scaffolding protein which causes the formation of caveolae through its association with cholesterol (yellow). The scaffolding domain of caveolin-1 (green) binds to the caveolin binding motif (red) of several intracellular signaling molecules (Gα subunits, eNOS, MAP kinases, Src kinases) resulting in the inhibition of downstream signaling.

Caveolin-1 mutations have been associated with human diseases such as cancer, diabetes, and atherosclerosis (Hnasko *et al.,* 2003). A large proportion of human breast and lung cancers have been linked to mutations in the CAV1 gene indicating caveolin-1 is involved in suppressing tumour development (Hayashi *et al.,* 2001; Racine *et al.,* 1999). Extensive work has been performed using abnormal caveolin-1 expression to study vascular system dysfunctions. These studies have linked abnormal caveolin-1 expression to cardiac hypertrophy, increased production of nitric oxide, defects in angiogenesis and atherosclerosis (Hnasko *et al.,* 2003).

The majority of research involving caveolin-1 has focused on associations with vascular diseases and cancer; however, evidence suggests this protein could also be involved in respiratory diseases, such as asthma. Caveolin-1 is expressed abundantly by lung cells, such as airway smooth muscle, the epithelium, and type I pneumocytes (Smart *et al.,* 1999). It is well established that epithelial cells and airway smooth muscle contribute to local inflammation via caveolae associated receptors for external signals such as growth factors and viral infection

(Halayko *et al.,* 2005). Secondly, caveolin-1 regulates receptor mediated airway smooth muscle cell responses through their association with G protein coupled receptors (Bergdahl *et al.,* 2004; Halayko *et al.,* 2005). These responses include contraction and proliferation, required for the development of airway hyperresponsiveness. A functional role for caveolae and caveolin-1 in the key cells that control airway responses and inflammation, suggests the protein could modulate important aspects of asthma pathogenesis and morbidity.

1.6 Caveolin-1 Knockout Mice

The recent availability of genetically engineered caveolin-1 knockout mice has provided the opportunity to study the *in vivo* role of this protein using whole animal models. The CAV1 gene is silenced by targeted disruption of exons 1 and 2, and results in the loss of caveolae in caveolin-1 knockout mice (Razani *et al.,* 2001a). When caveolin-1 is absent, the arrangement of cholesterol in lipid rafts is destabilized, leading to the loss of these structures (Dreja *et al.,* 2002; Galbiati *et al.,* 2001). Although caveolae are abundant in many different cells types, caveolin-1 knockout mice are viable and do not possess any developmental abnormalities (Razani *et al.,* 2001a). Nonetheless, Park *et al.* (2003) showed that caveolin-1 knockout mice show dramatic reductions in life span compared to homozygous and heterozygous animals. They concluded that major declines in viability occur between 27 and 65 weeks of age as a result of pulmonary fibrosis, pulmonary hypertension and cardiac hypertrophy (Park *et al.,* 2003).

As expected, caveolin-1 knockout mice show significant changes in their physiology. While caveolae differ from clathrin-coated pits, it has been shown that certain endocytotic events occur exclusively via caveolae. For example, albumin, certain glycosylphosphatidylinisotol (GPI) -anchored proteins and even some viruses are internalized via caveolae (Razani *et al.,* 2001a). Caveolin-1 knockout mice fail to show internalization of gold-conjugated albumin after perfusion, suggesting that no caveolae-associated endocytosis occurs in these mice (Schubert *et al.,* 2001). CAV1 is considered to be a tumour suppressor

gene because it inhibits the signaling activity of proto-oncogene products (Hnasko *et al.,* 2003; Macleod *et al.,* 1999). In cells derived from tissue (primary cells), the loss of caveolin-1 results in increased proliferation, indicating caveolin-1 normally inhibits mitogenic signaling pathways (Razani *et al.,* 2001c). As discussed previously, the scaffolding domain of caveolin-1 normally inhibits endothelial nitric oxide synthase (eNOS) signaling, resulting in the loss of vasodilatory responses in vivo (Bucci *et al.,* 2000). Consequently, caveolin-1 null vascular smooth muscle cells exhibit a several-fold increase in nitric oxide, resulting in the rapid loss of vascular tone (Drab *et al.,* 2001). Similarly, caveolin-1 null aortas show a blunted response to vasoconstrictive agents and exhibit an increase in acetylchloline-induced vasorelaxation (Drab *et al.,* 2001; Razani *et al.,* 2001c). Caveolin-1 is therefore important for normal vascular functions through control of smooth muscle cell responses.

The lung possesses an extraordinary abundance of caveolae, so it is not surprising that caveolin-1 null lungs show histological abnormalities. Caveolin-1 knockout mice show significantly smaller, or constricted alveolar spaces with thickened alveolar septa and hypercellularity (Drab *et al.,* 2001; Razani *et al.,* 2001c). Also, endothelial cells are significantly increased in knockout animals compared to wild type organisms, and cellular proliferation occurs to a greater extent in these mice (Razani *et al.,* 2001a). The loss of caveolae results in significant changes in lung structure; however, only preliminary research has been performed to study the physiological significance of these findings. For example, it has been shown that caveolin-1 knockout mice are easily fatigued following swimming (Drab *et al.,* 2001; Razani *et al.,* 2001c). The abundance of caveolae in the lung, their association with smooth muscle function and cell proliferation, and the histological abnormalities associated with the loss of caveolin-1, suggests a more rigorous assessment of lung physiology is required. This is a key focus of the current research project.

1.7 Hypothesis

In this study, I tested the hypothesis that the expression of caveolin-1 is a significant determinant, both of airway structure and function, and of inflammatory responses to inhaled allergic proteins that induce airway hyperresponsiveness. The first objective of the project was to develop an effective allergen sensitization and challenge protocol, capable of inducing acute airway inflammation and airway hyperresponsiveness in mice. Pilot studies were performed using BALB/c mice because previous research has shown these mice to be more responsive during lung function tests, following sensitization and challenge with allergen (Adler *et al.,* 2004; Henderson *et al.,* 2002; Whitehead *et al.,* 2003). The confirmed protocol was then used to sensitize and challenge caveolin-1 knockout and B6129SF2/J mice to determine the effect of caveolin-1 absence on acute allergen-induced airway hyperresponsiveness and inflammation. Finally, lung structure and function were characterized and compared between caveolin-1 knockout mice and B6129SF2/J mice.

Previous research involving caveolin-1 has focused on the cardiovascular system and cancer associations, though evidence suggests this protein may also be a significant determinant of airway structure and function. The identification of new mechanisms involving caveolin-1, which contribute to lung cell function and asthma pathogenesis, will be crucial in the development of more effective therapeutic agents for the treatment of the disease.

2. Materials and Methods

Experiments were performed using 3 mouse strains: BALB/c, B6129SF2/J, and Cav1^{tm1Mls}. BALB/c mice are commonly used to model allergic asthma since they show extreme responses to methacholine challenges following allergen sensitization and challenge (Henderson *et al.,* 2002; Khan *et al.,* 2002; Leigh *et al.,* 2002; Yang *et al.,* 1999). We used these mice to test our allergen sensitization and challenge protocol. Cav1^{tm1Mls} have the CAV1 gene disrupted and are commonly referred to as caveolin-1 knockout mice. B6129SF2/J mice were used as controls in our experiments. These mice retain normal caveolin-1 expression and are the closest commercially available genetic control for the caveolin-1 knockout mouse. All animals were used in accordance with the guidelines issued by the Canadian Council on Animal Care, and all animal care utilization protocols were approved by the Animal Care Committee at the University of Manitoba.

2.1 Allergen Sensitization and Challenge Protocol

The allergen sensitization and challenge protocol was developed based on successful protocols used by several researchers (Henderson *et al.,* 2002; Khan *et al.,* 2002; Leigh *et al.,* 2002; Yang *et al.,* 1999). Mice were sensitized intraperitoneally (*i.p.*) with 500µl of ovalbumin (2µg per mouse) (Sigma Aldrich; catalogue # A5503-10G) in 4 mg of $Al(OH)_3$ adjuvant (Alum Inject; Pierce Chemical; catalogue # 77161) on Day 1 and Day 8. Following sensitization, mice were challenged with 50µl of intranasal ovalbumin (50 µg per mouse) on Day 12 and Day 15 (Figure 3). Animals were briefly anesthetised using isofluorane gas prior to injections and intranasal exposures. Lung function measurements and bronchoalveolar lavages were performed prior to sensitization, following sensitization, and following challenge (Figure 3). For details of these procedures see sections 2.2 and 2.3.

To test if the allergen sensitization and challenge protocol induces inflammation and methacholine hyperresponsiveness, pilot studies were performed using BALB/c mice. Female BALB/c mice, aged 6-8 weeks were purchased from Central Animal Care at the

University of Manitoba and were treated using two protocols: experimental and control. Experimental mice were sensitized and challenged with ovalbumin, while control mice received filter-sterilized saline in place of ovalbumin.

Female caveolin-1 knockout mice and B6129SF2/J mice, aged 6-8 weeks, were purchased from The Jackson Laboratory (Bar Harbour, ME) after completion of the pilot studies. Due to the limitations of order size, a saline control group was not performed, thus both strains of mice were sensitized and challenged with ovalbumin. Lung tissue was collected prior to sensitization for histology (section 2.4). Data analysis focused on the difference in lung structure, function and inflammation due to the presence or absence of caveolin-1.

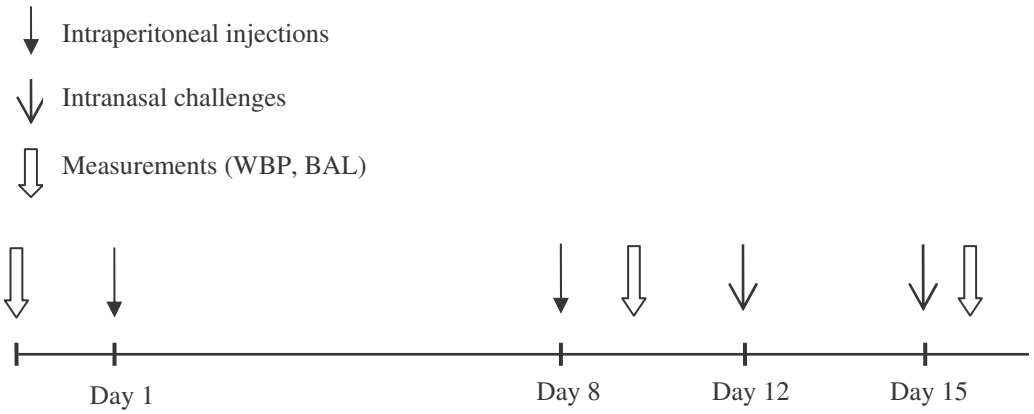

Figure 3: Allergen sensitization and challenge protocol. Mice were sensitized by intraperitoneal injections on days 1 and 8 and challenged by intranasal exposures on days 12 and 15. Lung function tests (WBP) were performed on day 0, day 10 and day 16 and bronchoalveolar lavages (BAL) on day 0, day 11 and day 17. Lung tissue was collected from the caveolin-1 knockout mice and B6129SF2/J mice only on day 0.

2.2 Whole Body Plethysmography (WBP)

Lung Function was measured by whole body plethysmography in live unrestrained animals and expressed as enhanced pause (Penh). Penh is a calculated value which reflects the pulmonary resistance experienced by the animals and was measured by a conventional, two chamber plethysmograph purchased from Buxco Electronics, Inc (Troy, NY). Enhanced

pause is derived from changes in the box pressure induced by bronchoconstriction during peak expiratory pressure (PEP) and peak inspiratory pressure (PIP) (Figure 4).

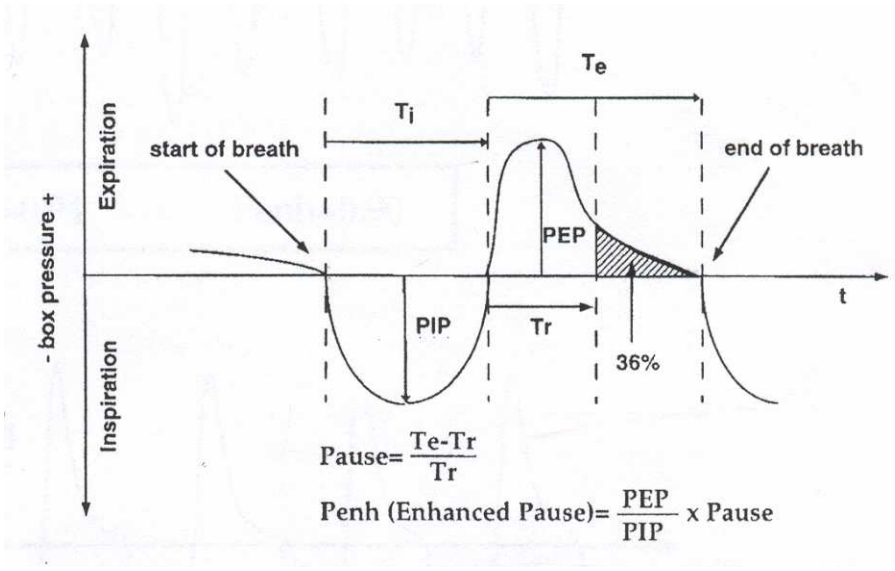

Figure 4: Schematic of a box pressure wave explaining the calculation of enhanced pause (Penh). T_i = inspiration time (s): the time from start of inspiration to the end of inspiration; Te = expiration time (s): the time from end of inspiration to start of next inspiration; T_r = relaxation time (s): time of the pressure decay to 36% of the total box pressure during expiration; PIP = peak inspiratory pressure (ml/s): maximal negative box pressure occurring in one breath; PEP = peak expiratory pressure (ml/s): maximal positive box pressure occurring in one breath. Pause reflects the timing of expiration.(Hamelmann *et al.,* 1997)

The methacholine dose response curves were performed using a Buxco aerosol delivery system (Buxco Electronics Inc., Troy, NY). The system includes a "push" bias flow regulator that provides a flow of fresh air through the animal chambers to minimize CO_2 levels. Methacholine was aerosolized using an ultrasonic nebulizer, an aerosol controller, and an aerosol distribution chamber. The settings for dilution flows and aerosol time period were selected according to the manufacturer's recommendations. All the signals were filtered by a MAX II unit preamplifier, and the data were obtained and stored using Biosystem XA software for Windows (Figure 5).

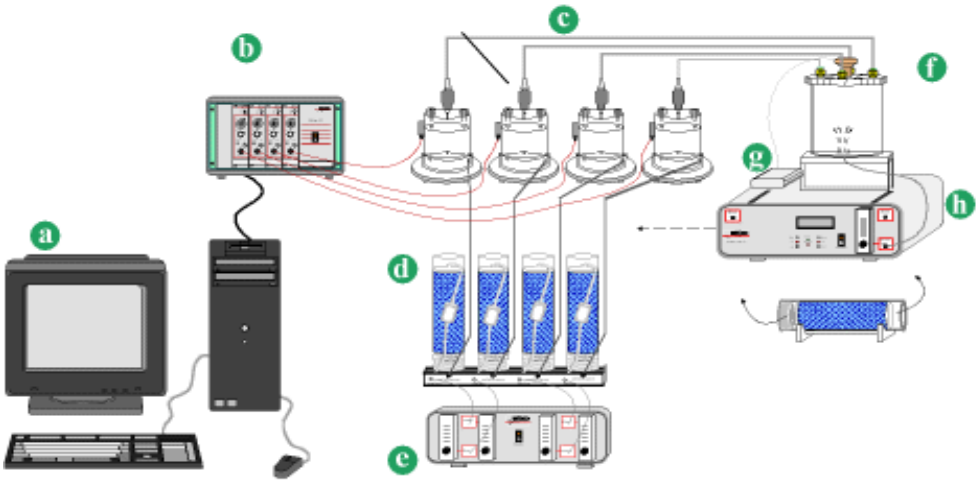

Figure 5: Buxco whole body plethysmograph system set up. a= Biosystem XA Data Acquisition Software for Windows; b= MAX II preamplifier unit; c= Whole Body Unrestrained Plethysmographs; d= Drying Stand; e= Bias Flow Regulator; f= Aerosol Distribution Chamber; g= Aerogen Nebulizer; h= Nebulizer Controller (Buxco manual).

To measure the breathing response to increasing concentrations of inhaled methacholine, mice were placed into the individual chambers of the plethysmograph and were acclimatized for 10 minutes. Methacholine solutions (Sigma; catalogue # A2251-100G) were prepared by serial dilution to obtain concentrations ranging from 3.1 mg/ml to 50mg/ml (Appendix 6.1.1). Following acclimatization, baseline lung function measurements were taken for 5 minutes. The mice were then exposed to 400 µl of aerosolized saline for 3 min and then to increasing concentrations of aerosolized methacholine with an ultrasonic nebulizer (Aerogen Inc., Hackensack NJ). Recordings were taken for 5 minutes after each nebulization. The Penh values measured during this recording period were averaged and obtained using Biosystem Data Export software to Excel.

2.3 Bronchoalveolar Lavage and Cell Differentials

Twenty four hours following lung function tests, (day 0, 11 and 17 of sensitization and challenge protocol) animals were euthanized using 200 µl of 16.4 mg/ml Somnitol (MTC Pharmaceuticals, Hamilton, ON).

2.3.1 Bronchoalveolar lavage (BAL)

Following anaesthesia, the trachea was cannulated with a 20 gauge catheter and tied in place. A syringe with 1 ml of ice cold saline was attached to the catheter and the saline was injected and retrieved twice. The lungs were washed with another 1 ml of ice cold saline for a total of 2 ml. Approximately 90% of the fluid was recovered.

The bronchoalveolar lavage fluid (BALF) was centrifuged at 1000 rpm for 10 minutes and the pellet was resuspended in 500 μl of ice cold saline. Total cell counts were determined using a hemocytometer and solutions were diluted to approximately 300,000 cells/ml. Cells were fixed to slides using a Cytospin® 3 from Shandon Inc. (1000 rpm for 5 minutes) and stained with the Hema 3® Stat Pack (Fisher Scientific Co; catalogue # 123-869) modified Wright-Giemsa stain as per manufacturer's instructions.

2.3.2 Cell differentials

Slides of BALF cells were examined under 40x magnification using an Olympus light microscope. Six randomly chosen fields of view were selected and macrophages, lymphocytes, eosinophils, and neutrophils were counted in each field of view. Individual cell types were identified on the basis of cell morphology as per instructions provided in the Hema 3® Stat Pack staining kit. Cell counts were performed independently by two people. Counts were totalled across the six fields of view and expressed as percentage of total BALF cells.

2.4 Histology

Lungs were harvested from naïve caveolin-1 knockout and B6129SF2/J mice and fixed overnight in formalin (Fisher Scientific; catalogue # 305-510). Tissues were processed using the protocol described in Table 1 using a Citadel® Tissue Processor from Shandon Inc. Left and right lungs were separated and embedded separately in paraffin wax.

Table 1: Procedure for Processing Lung Tissue

Step	Solution	Time
1	70% ethanol	4 hours
2	70% ethanol	4 hours
3	80% ethanol	4 hours
4	95% ethanol	2 hours
5	95% ethanol	2 hours
6	100% ethanol	2 hours
7	100% ethanol	2 hours
8	100% ethanol/xylene	20 minutes
9	Xylene	20 minutes
10	Xylene	20 minutes
11	Paraffin wax	2 hours
12	Paraffin wax	2 hours

The lungs were sectioned using a Microtome sectioner (Shandon Inc.). Sections 6μm thick were placed on slides with three sections per slide. The slides were incubated overnight at 37ºC to fix the sections to the slide.

2.4.1 Deparaffinization and Rehydration

Prior to any staining, lung sections underwent processes to remove the paraffin wax and rehydrate the tissue. The protocols for deparaffinization and rehydration are described in Table 2.

Table 2: Procedures for Deparaffinization and Rehydration

Step	Solution	Time
Deparaffinization		
1	xylene	10 minutes
2	xylene	10 minutes
Rehydration		
1	100% ethanol	3 minutes
2	90% ethanol	3 minutes
3	80% ethanol	3 minutes
4	70% ethanol	3 minutes
5	Distilled water	unlimited

2.4.2 Hematoxylin and Eosin (H&E) Stain

H&E stain was used to reveal general cellular composition and to clearly identify epithelium and airway smooth muscle. Prior to staining, slides underwent deparaffinization and rehydration. The majority of the water was removed from the slides and slides were placed in Harris Modified Hematoxylin (Fisher Scientific; catalogue # SH26-500D) for 3

minutes. Slides were flushed under running distilled water for 10 minutes and then placed in 1% HCl in 70% ethanol for 20 seconds. Slides were removed and placed in distilled water for approximately 15 minutes until tissue turned blue, following which they were removed and placed in Alcoholic Eosin Yellowish Solution (Fisher Scientific; catalogue # SE22-500D) for 5 minutes. Slides were rinsed with 3-5 dips in distilled water, dehydrated and cleared.

2.4.3 Masson's Trichrome Stain

Masson's Trichrome staining was used to visualize fibrotic tissue in the airways. Prior to staining, slides were deparaffinized and rehydrated. Slides were allowed to mordant in preheated Bouin's solution (Sigma Aldrich; catalogue # HT-10-1-32) at 56ºC for 30 minutes. During this time, Wiegert's Iron Hematoxylin(Sigma-Aldrich; catalogue # HT1079-1SET) and Phosphotungstic/Phosphomolybdic acid solutions(Sigma-Aldrich; catalogue # HT15-1KT) were prepared following manufacturer's instructions (Appendix 6.1.2 and 6.1.3). After incubation in Bouin's solution, the slides were cooled in tap water for 5 minutes and then flushed under running tap water to remove the yellow colour from the tissue sections. Slides were placed in Wiegert's Iron Hematoxylin for 10 minutes, flushed under running tap water for 10 minutes and then rinsed in distilled water. Slides were stained in Biebrich Scarlet-Acid Fucshin (Sigma-Aldrich; catalogue # HT15-1KT) for 15 minutes, and then rinsed in distilled water. Slides were then placed in working Phosphotungstic/Phosphomolybdic acid solution for 5 minutes, followed by aniline blue (Sigma-Aldrich; catalogue # HT15-1KT) for 7 minutes. Slides were placed in 1% acetic acid for 5 minutes, rinsed in distilled water, dehydrated and cleared.

2.4.4 Dehydration and clearing

Table 3: Procedures for Dehydration and Clearing

Step	Solution	Time
Dehydration		
1	70% ethanol	2 minutes
2	80% ethanol	2 minutes
3	90% ethanol	2 minutes
4	100% ethanol	2 minutes
Clearing		
1	Xylene	2 minutes
2	Xylene	2-5 minutes

2.4.5 Image analysis

Slides were photographed and viewed under 20x and 40x magnification, using a Nikon light microscope equipped with Image Pro image analysis software. An assessment of the morphological differences seen in the airways of caveolin-1 knockout mice and B6129SF2/J mice was performed focusing on the appearance of the airway smooth muscle and the epithelium, the level of fibrosis, and the differences in alveolar structure.

2.5 Statistical Analysis

All statistical analysis was performed using Graphpad Prism software (version 3.03). Data are presented as the means ± SE. Statistical analysis was performed using one-way analysis of variance (ANOVA) and Tukey's Honestly Significantly Different (HSD) Post Hoc test. Differences between means were considered significant when $P<0.05$.

3. Results

3.1 BALB/c Mice Experiments

3.1.1 Lung Function

Our pilot studies showed that the ovalbumin sensitization and challenge protocol was effective at producing methacholine (MCh) hyperresponsiveness in ovalbumin sensitized and challenged BALB/c mice (OVA group). MCh hyperresponsiveness was not observed in the Saline group that was sensitized and challenged with only saline. The changes in lung function were detected through whole body plethysmography (WBP) and expressed as mean Penh± SE. Figure 6 shows the increases in Penh response following methacholine exposure in OVA and Saline experimental groups. The control group (Saline) showed small dose dependent increases in Penh in response to aerosolized MCh. In contrast, the mice that were sensitized and challenged with allergen (OVA) showed a significantly larger increase in Penh following MCh exposure compared with the control mice. The baseline Penh measurements (OVA 1.06 ± 0.15, Saline 1.15 ± 0.07) and measurements following exposure to aerosolized saline (OVA 1.20 ± 0.03, Saline 1.34 ± 0.09) were similar in both groups. The measurements at lower doses of MCh were also similar between groups; however, at higher doses of MCh, the differences in Penh response between groups became more prominent (50mg/ml: OVA 33.28 ± 9.06, Saline 4.15 ± 0.26). These data indicate that Penh values are increased in allergen-sensitized and challenged mice at higher doses of MCh and therefore, the allergen sensitization and challenge protocol is capable of inducing airway hyperresponsiveness.

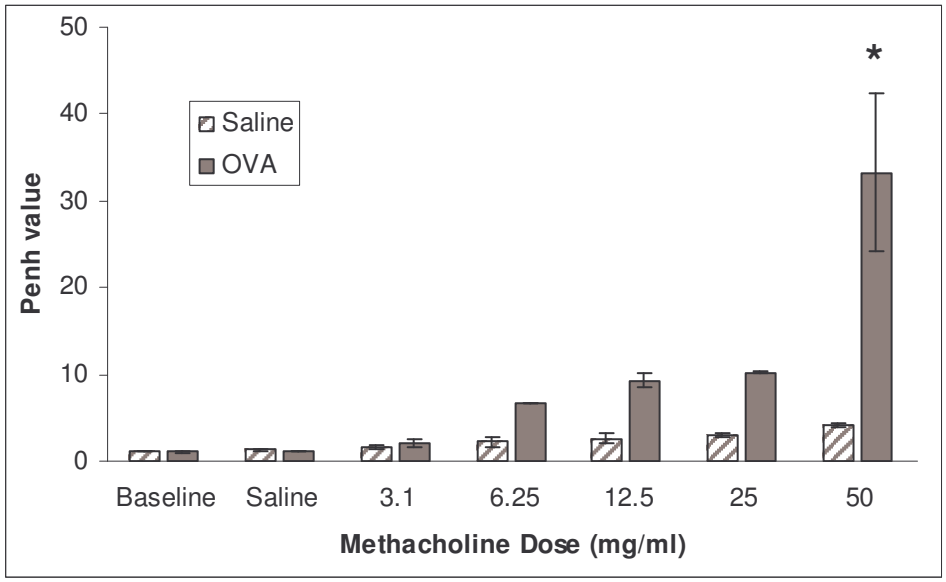

Figure 6: Penh response in allergen and saline sensitized and challenged BALB/c mice. Animals were sensitized with OVA/alum or saline *i.p.* on Days 1 and 8 and challenged intranasally with OVA or saline on Days 12 and 15. Lung function was measured by unrestrained whole body plethysmography on Day 16 (shown here). The OVA sensitized and challenged group (OVA, n=2) and the saline sensitized and challenged group (Saline, n=2) are compared. Penh values are expressed as the mean ± SE. Sensitization and challenge with OVA induces a significantly higher Penh response at 50mg/ml MCh (*P< 0.001).

To compare the effects of sensitization and challenge at each stage of the allergen protocol, the Penh values at the 50mg/ml dose of MCh were compared between the OVA and Saline groups (Figure 7). The changes in lung function at the 50 mg/ml dose were measured by whole body plethysmography and expressed as mean Penh value ± SE. The control group (Saline) showed no significant increase in Penh at the 50mg/ml dose of MCh when compared on Day 0 (prior to sensitization) (4.36 ±1.20), Day 10 (following sensitization with saline *i.p.*)(3.61 ± 0.82) and Day 16 (following intranasal challenge with saline) (4.15 ± 0.26) (P>0.05). The experimental group (OVA) showed no significant increase in Penh at the 50 mg/ml dose of MCh when compared on Day 0 (4.44 ± 1.27) and Day 10 (following sensitization with OVA)(4.68 ± 0.03)(P>0.05). However, there was a significant increase in Penh response following intranasal challenge with OVA on Day 16 (33.28 ± 9.06)(P<0.001). These data indicate that sensitization alone is not sufficient to induce methacholine hyperresponsiveness in response to inhaled 50mg/ml MCh. However, with the

induction of acute airway-specific allergen exposure, a profound increase in lung resistance develops in response to inhaled methacholine.

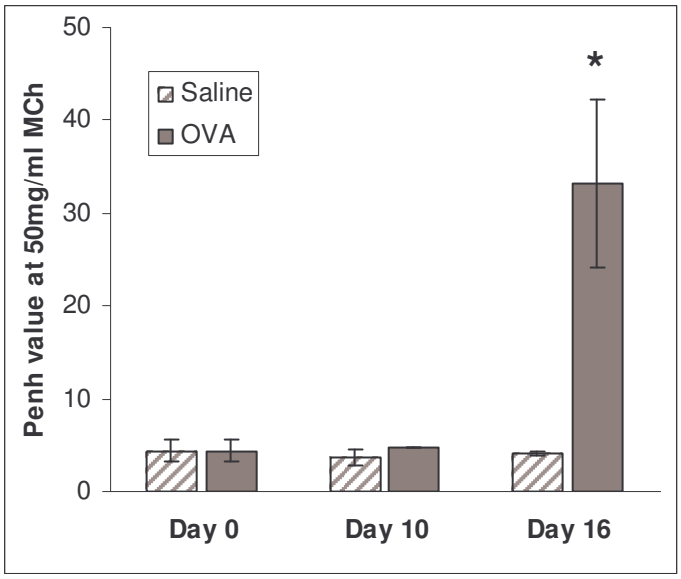

Figure 7: Effect of allergen sensitization and challenge on maximum Penh response in BALB/c mice. Penh values for the 50 mg/ml MCh dose are compared between the OVA sensitized and challenged group (OVA, n=2 for each time point) and the saline sensitized and challenged group (Saline, n=2 for each time point). Comparisons are made prior to sensitization on Day 0, after sensitization on Day 10, and after challenge on Day 16. Penh values are expressed as the mean ± SE. Allergen sensitization and challenge with OVA induced MCh hyperresponsiveness on Day 16 (*P<0.001).

3.1.2 Bronchoalveolar lavage fluid (BALF) cell differentials

BALF cell differentials did not differ in the experimental groups for BALB/c mice until after intranasal challenges were completed. Only half of the experimental animals were lavaged, resulting in an n=1 for each group in these pilot studies. The BALB/c mice were used to identify any trends in changes to BALF cells: prior to sensitization, following sensitization with OVA or Saline and following intranasal challenges with OVA or Saline. There was no significant difference in BALF cell counts between groups prior to sensitization and after sensitization (data not shown).

Prior to sensitization (Day 0), the number of eosinophils (Figure 8A) and neutrophils (Figure 8B) in the BALF of both experimental groups was minimal (OVA eosinophils 0%, Saline eosinophils 0%, OVA neutrophils 0.81%, Saline neutrophils 1.61%). Conversely,

macrophages (Figure 8D) made up the majority of the BALF cells in both groups (OVA 95.16%, Saline 96.77%). After intranasal challenge (Day 17), the profile of inflammatory cells in the BALF of the OVA group changed markedly. Eosinophils were especially high, constituting 76.37% of the cells in the BALF of the OVA treated group (Figure 8A). Neutrophils also increased following OVA intranasal challenge, making up 20.55% of the BALF cells in these mice (Figure 8B). There was no significant increase in either eosinophil (0.35%) or neutrophil (1.06%) cell counts in the Saline group. Macrophage cell counts decreased following OVA intranasal challenge (1.96%), though this was not the case in the Saline group, as macrophages continued to make up 95.77% of the total BALF cells in these mice (Figure 8D). Throughout the allergen sensitization and challenge protocol, the percentage of lymphocytes in the BALF in both experimental groups showed no significant differences (Figure 8C).

These data suggest that OVA sensitization and challenge results in airway inflammation marked by increased eosinophilia in BALB/c mice. Notably, this trend is entirely consistent with numerous published reports using OVA-challenged BALB/c mice (Henderson *et al.,* 2002; Leigh *et al.,* 2002). Collectively, these data suggest the protocol that has been developed for my studies effectively induces acute airway inflammation with a corresponding increase in responsiveness to inhaled methacholine.

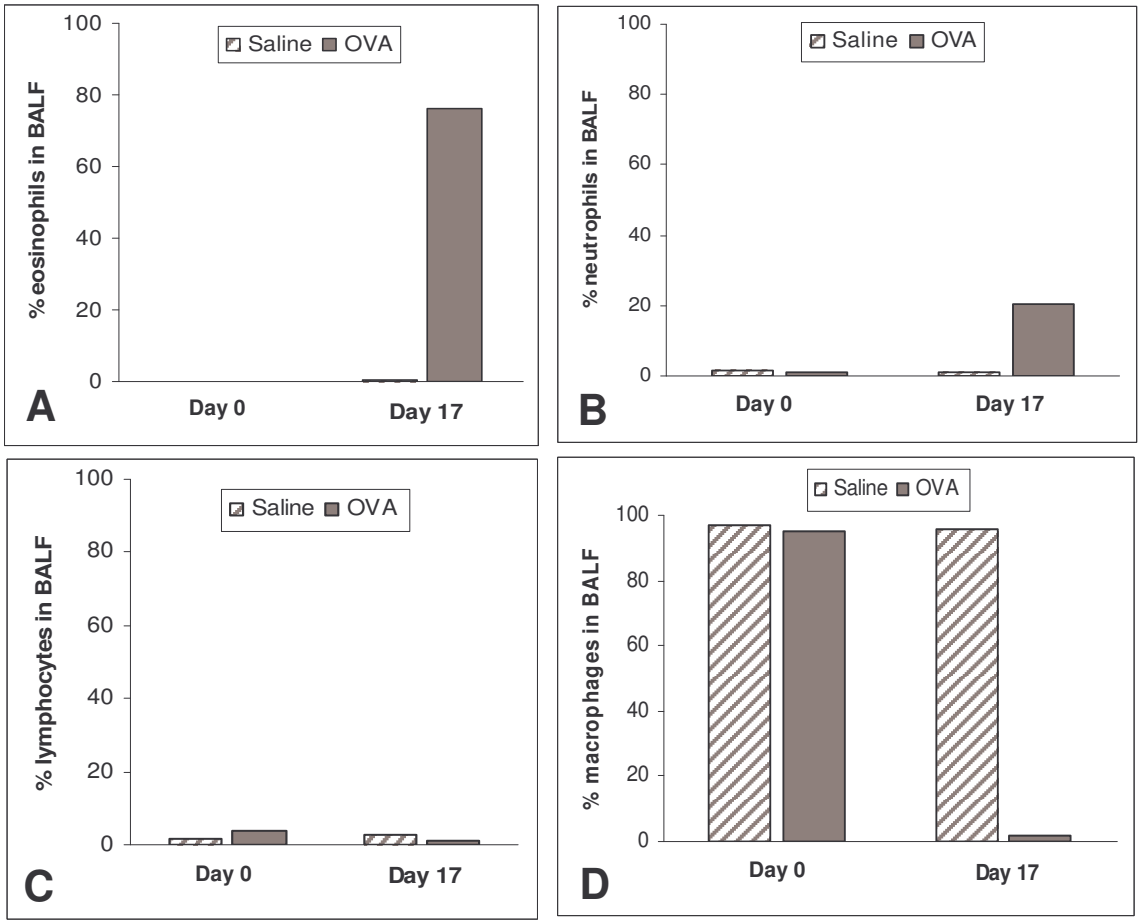

Figure 8: Effect of allergen sensitization and challenge on BALB/c bronchoalveolar lavage fluid (BALF) cell differentials. BALF cell differentials are compared between the OVA sensitized and challenged group (OVA, n=1) and the saline sensitized and challenged group (Saline, n=1). BALF was collected prior to sensitization (Day 0), after sensitization with OVA or saline (Day 11) and after intranasal challenge with OVA or saline (Day 17). There was no difference in the BALF cell counts prior to and after sensitization (data not shown). OVA sensitization and challenge increased the percentage of inflammatory cells in the BALF (eosinophils **(A)** and neutrophils **(B)**) and decreased the percentage of macrophages **(D)**. OVA sensitization and challenge had no effect on the percentage of lymphocytes in the BALF **(C)**.

3.2 Caveolin-1 Knockout Mice Experiments

3.2.1 Lung Function

Allergen sensitization and challenge did not produce the methacholine (MCh) hyperresponsiveness seen in BALB/c mice in either the caveolin-1 knockout (Cav-1 KO) animals or the genetic control strain (B6129SF2/J). Lung function was measured by whole body plethysmography and expressed as mean Penh ± SE. Figure 9 shows the increases in Penh response following methacholine exposure in Cav-1 KO and B6129SF2/J mice.

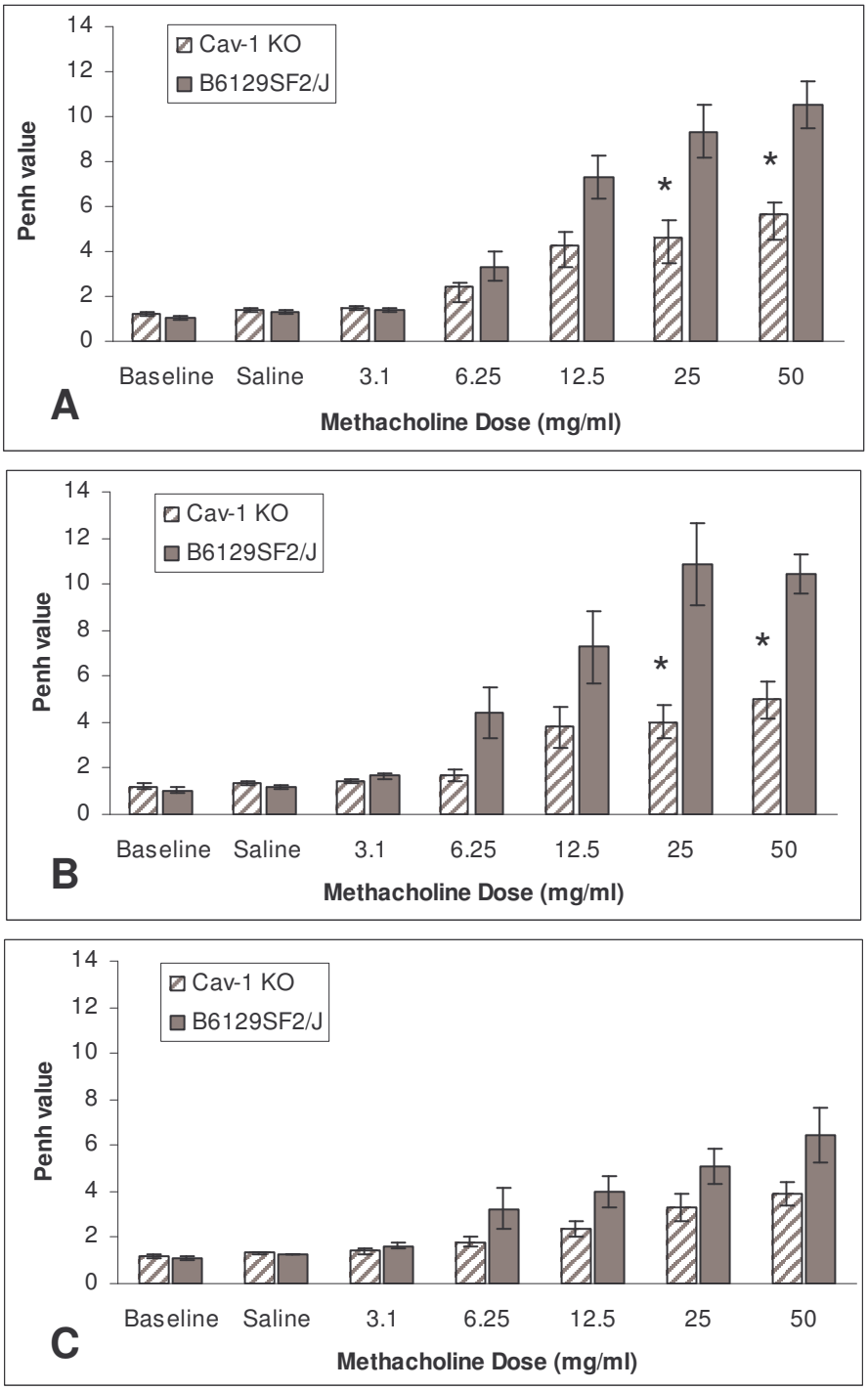

Figure 9: Penh response in caveolin-1 knockout (Cav-1 KO) and genetic control (B6129SF2/J) mice before and after OVA sensitization and challenge. Lung function was measured by whole body plethysmography and is represented mean Penh ± SE. Comparisons are made between Cav-1 KO and (B6129SF2/J) prior to sensitization (Cav-1 KO n=10; B6129SF2/J n=10)**(A)**, after sensitization (Cav-1 KO n=8; B6129SF2/J n=8)**(B)**, and after intranasal challenge (Cav-1 KO n=8; B6129SF2/J n=7)**(C)**.

Prior to and after allergen sensitization, Cav-1 KO mice are significantly hyporesponsive at higher doses of MCh (*P<0.01). Cav-1 KO mice remain hyporesponsive to MCh following OVA sensitization and challenge compared to the genetic control strain though not statistically significant (P>0.05). Allergen sensitization and challenge did not induce MCh hyperresponsiveness in either strain. Prior to any treatment (Figure 9A) the Cav-1 KO mice showed smaller MCh dose dependent increases in Penh, compared to the genetic control strain. Conversely, B6129SF2/J mice showed significantly larger increases in Penh after MCh exposure. The two mouse strains were not significantly different during the baseline measurements or after exposure to saline. The measurements at lower doses of MCh were similar between mouse strains, and differences did not become clear until higher doses were administered. At this point, Penh values were ~50% lower in the Cav-1 KO mice (25 mg/ml 4.63 ± 0.76, 50 mg/ml 5.61 ± 0.57) compared to B6129SF2/J mice (25 mg/ml 9.32 ± 1.17, 50mg/ml 10.53 ± 1.07). This pattern is very similar to that of the BALB/c mice, indicating that the higher doses of MCh are more useful in distinguishing differences between groups.

Following sensitization, (Figure 9B) the difference in Penh values between mouse strains was maintained at the 25mg/ml (Cav-1 KO 4.01 ± 0.72, B6129SF2/J 10.85 ± 1.82) and 50mg/ml (Cav-1 KO 4.97 ± 0.83, B6129SF2/J 10.44 ± 0.86) MCh doses. There was no significant increase in Penh response in either mouse strain after sensitization compared to the baseline measurements (Figure 10). Again this suggests that sensitization alone is not sufficient at producing airway hyperresponsiveness.

Following allergen sensitization and challenge with OVA (Figure 9C), neither mouse strain appeared to be hyperresponsive to MCh. This is in contrast to the results in the BALB/c experiments. In fact, the Penh response in both the caveolin-1 knockout and genetic control mice were reduced at the 50mg/ml dose of MCh after sensitization and challenge. Compared to the Penh values prior to treatment and after *i.p.*'s, the B6129SF2/J

mice showed significantly smaller Penh values at the 50mg/ml MCh dose after allergen challenge ($P<0.05$)(Figure 10). Cav-1 KO mice showed a similar trend, but this was not statistically significant ($P>0.05$)(Figure 10).

The overall difference in Penh response between Cav-1 KO and B6129SF2/J mice was reduced and found to be statistically insignificant after allergen sensitization and challenge ($P>0.05$) (Figure 9C and Figure 10). At the 25 mg/ml and 50mg/ml doses of MCh, the difference between mouse strains was found to be statistically insignificant even though Cav-1 KO mice (25 mg/ml 3.33 ± 0.58, 50 mg/ml 3.91 ± 0.49) still showed Penh values ~50% lower compared to the genetic control mice (25mg/ml 5.09 ± 0.75, 50 mg/ml 6.44 ± 1.19).

These data indicate there is an intrinsic difference in caveolin-1 knockout mice that results in hyporesponsiveness to MCh during lung function tests. Allergen sensitization and challenge did not induce MCh hyperresponsiveness in either mouse strain as was seen in BALB/c mice (Figure 10). In fact, allergen sensitization and challenge decreased overall Penh response in both mouse strains and the difference between strains at all doses of MCh were not statistically significant ($P>0.05$).

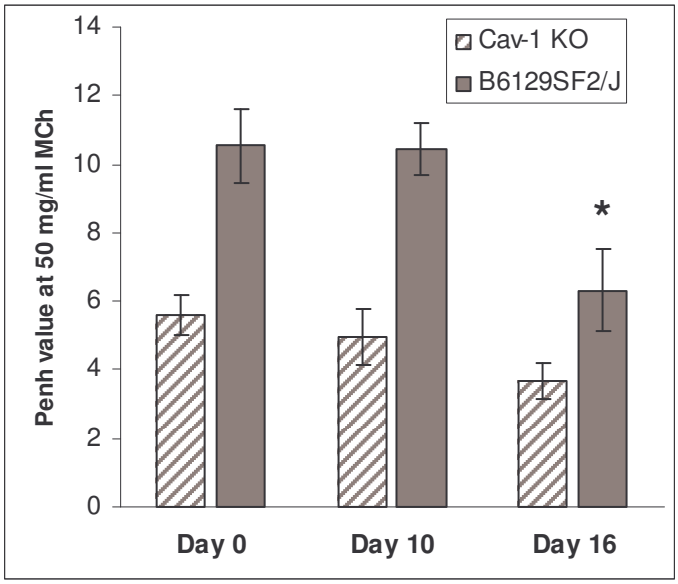

Figure 10: Comparison of maximum Penh response after allergen sensitization and challenge in caveolin-1 knockout and B6129SF2/J mice. Penh values for the 50 mg/ml MCh dose are compared between caveolin-1 knockout mice (Cav-1 KO) and genetic control mice (B6129SF2/J). Comparisons are made prior to sensitization on Day 0 (Cav-1 KO n=10, B6129SF2/J n=10), after sensitization with OVA on Day 10 (Cav-1 KO n=8, B6129SF2/J n=8), and after challenge on Day 16 (Cav-1 KO n=8, B6129SF2/J n=7). Penh values are expressed as the mean ± SE. Allergen sensitization and challenge did not induce MCh hyperresponsiveness in either mouse strain as was seen in BALB/c mice. Maximum Penh response was significantly less in the genetic control mice after challenge with OVA (*P<0.05).

3.2.2 Bronchoalveolar lavage fluid (BALF) cell differentials

Genetic control mice (B6129SF2/J) showed a similar pattern of cell inflammation to that seen in OVA treated BALB/c mice (Figure 11). BALF cell differentials did not differ between mouse strains until after OVA intranasal challenges were completed. Only half of the experimental animals were lavaged, reducing the number of animals in each group, at each time point to n=4. Only 3 B6129SF2/J animals were lavaged after intranasal challenge due to a death. Data are expressed as percentage of cells in BALF ± SE.

Similar to the BALB/c mice, prior to sensitization (Day 0), the number of inflammatory cells in the BALF of both mouse strains was minimal. Eosinophils (Figure 11A) made up 1.35 ± 0.99% of the B6129SF2/J BALF cells and 0.25 ± 0.16% of the caveolin-1 knockout (Cav-1 KO) BALF cells. Similarly, neutrophils (Figure 11B) made up 0.39 ± 0.14% of the B6129SF2/J BALF cells and 0.19 ± 0.14% of the Cav-1 KO BALF cells. Macrophages

(Figure 11C) were the most abundant cell type found in the BALF of both mouse strains prior to sensitization (B6129SF2/J 87.63 ± 2.36% and Cav-1 KO 88.78 ± 2.29%).

Following sensitization with OVA *i.p.* (Day 11) there was no significant increase or decrease in the BALF cell counts compared to baseline measurements. Eosinophil (Cav-1 KO 1.24 ± 0.61% and B6129SF2/J 1.87 ± 0.53%) and neutrophils (Cav-1 KO 0.89 ± 0.33% and B6129SF2/J 2.10 ± 0.55%) levels remained low and macrophage levels (Cav-1 KO 90.5 ± 3.9% B6129SF2/J 85.1 ± 2.9%) remained high in both mouse strains (Figure 11 A B C).

After intranasal challenge (Day 17), the percentage of inflammatory cells in both the Cav-1 KO and B6129SF2/J BALF increased. This increase was found to be statistically significant only in the B6129SF2/J BALF ($P<0.001$). Though a similar trend appeared for Cav-1 KO mice, there was no statistically significant increase in the percentages of inflammatory cells on Day 17. The percentage of inflammatory cells in the Cav-1 KO BALF was significantly different compared to the B6129SF2/J BALF ($P<0.01$). For example, eosinophils (Figure 11A) were especially high in the B6129SF2/J BALF (53.46 ± 10.80%) compared to the Cav-1 KO BALF (20.72 ± 8.96%)($P<0.01$). Neutrophils (Figure 11B) were also increased on Day 17 in the B6129SF2/J BALF (20.52 ± 3.71%) compared to the Cav-1 KO BALF (5.24 ± 2.67%)($P<0.001$). Macrophage cell counts (Figure 11C) significantly decreased following OVA challenge in B6129SF2/J BALF (11.53 ± 2.93%)($P<0.001$); whereas, in Cav-1KO BALF, macrophages made up the highest percentage of BALF cells (68.57 ± 10.67%). This resulted in a significant difference in macrophage cell counts between caveolin-1 knockout mice and genetic controls ($P<0.001$). As in the BALB/c mice, there were no significant differences in lymphocyte cell counts (Figure 11D) between the knockouts and controls at any stage in the sensitization and challenge protocol.

These data suggest that OVA sensitization and challenge induced mainly eosinophilic airway inflammation in the genetic control mice. This was not the case in the knockouts,

suggesting that the inflammatory response may occur to a lesser extent, or the kinetics of the inflammatory response is altered in caveolin-1 knockout animals.

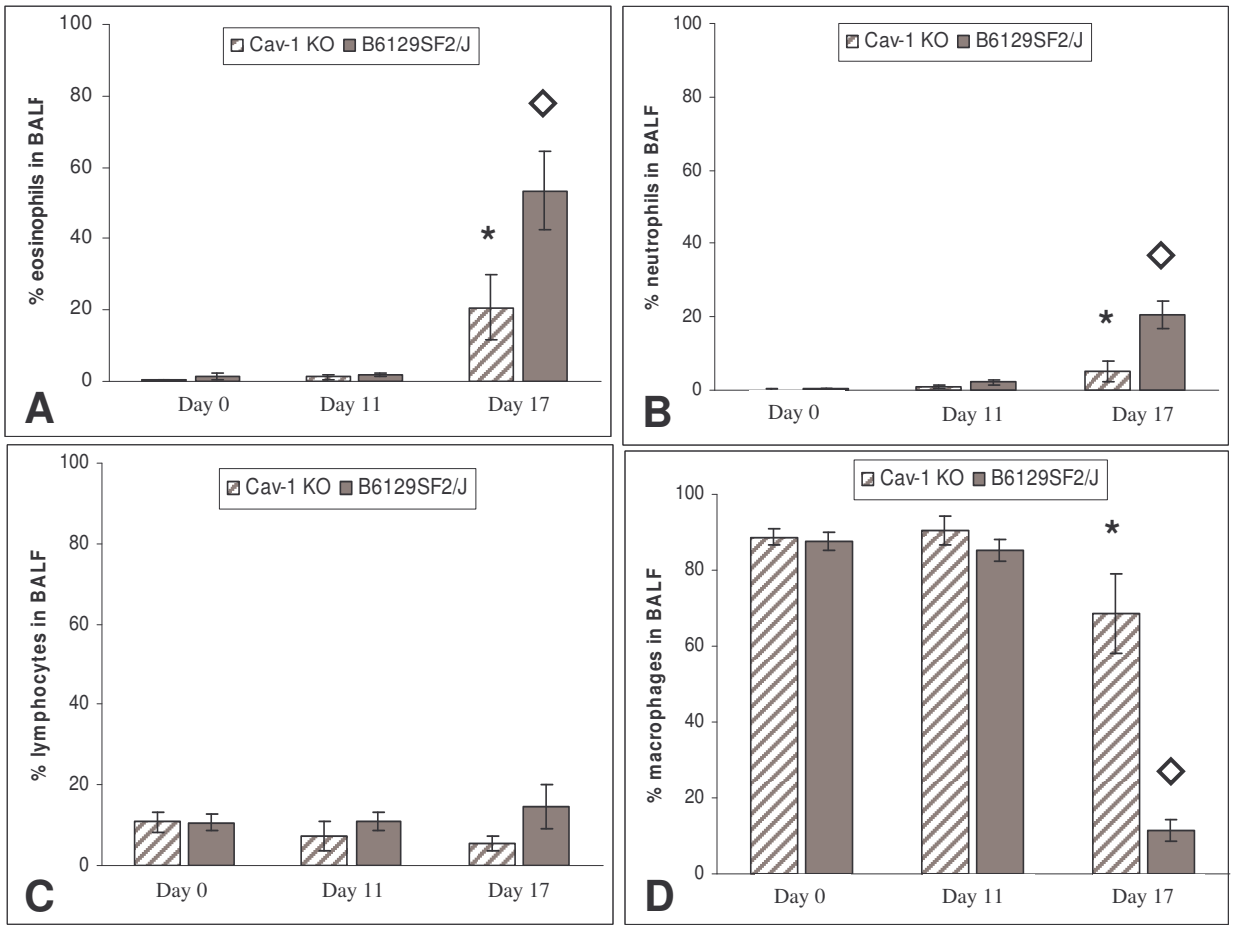

Figure 11: Effect of OVA sensitization and challenge on caveolin-1 knockout (Cav-1 KO) and B6129SF2/J bronchoalveolar lavage fluid (BALF) cell differentials. BALF was collected prior to sensitization (Day 0)(Cav-1 KO n=4; B6129SF2/J n=4), after OVA sensitization (Day 11)(Cav-1 KO n=4; B6129SF2/J n=4), and after OVA intranasal challenges (Day 17)(Cav-1 KO n=4; B6129SF2/J n=3). There were no significant differences in the BALF cell counts prior to and after sensitization in either mouse strain (Day 0 vs. Day 11). Allergen sensitization and challenge (Day 0 vs. Day 17) significantly increased the percentage of inflammatory cells in the B6129SF2/J BALF (eosinophils **(A)** and neutrophils **(B)**)(◇ $P<0.001$). The increase in inflammatory cells in Cav-1 KO BALF on Day 17 was not statistically significant. However, the percentage of eosinophils and neutrophils in the Cav-1 KO BALF were significantly different from the percentages of the same cells in the B6129SF2/J mice BALF (*$P<0.01$). Allergen sensitization and challenge had no significant effect on the percentage of lymphocytes in the BALF of either mouse strain **(C)**($P>0.05$). Allergen sensitization and challenge (Day 0 vs. Day 17) significantly decreased the percentage of macrophages **(D)** in the B6129SF2/J BALF (◇$P<0.001$). The percentage of macrophages in the caveolin-1 knockout mice BALF were significantly different from the percentages of the same cells in the B6129SF2/J mice BALF (*$P<0.001$).

3.2.3 Histology

Lung tissue was collected from both mouse strains prior to OVA sensitization to compare lung structure between caveolin-1 knockout mice and controls (B6129SF2/J). Lung sections, 6μm thick, were stained with Hematoxylin and Eosin (H&E) to observe general airway and peripheral lung components. H&E stain results in dark purple nuclei while different tissue components stain various shades of pink.

Considerable differences were detected when the airways from caveolin-1 knockout mice were compared to the airways from B6129SF2/J mice (Figure 12). Airways from caveolin-1 knockout mice showed a thickened, folded epithelium and a thicker airway smooth muscle layer compared to airways from B6129SF2/J animals.

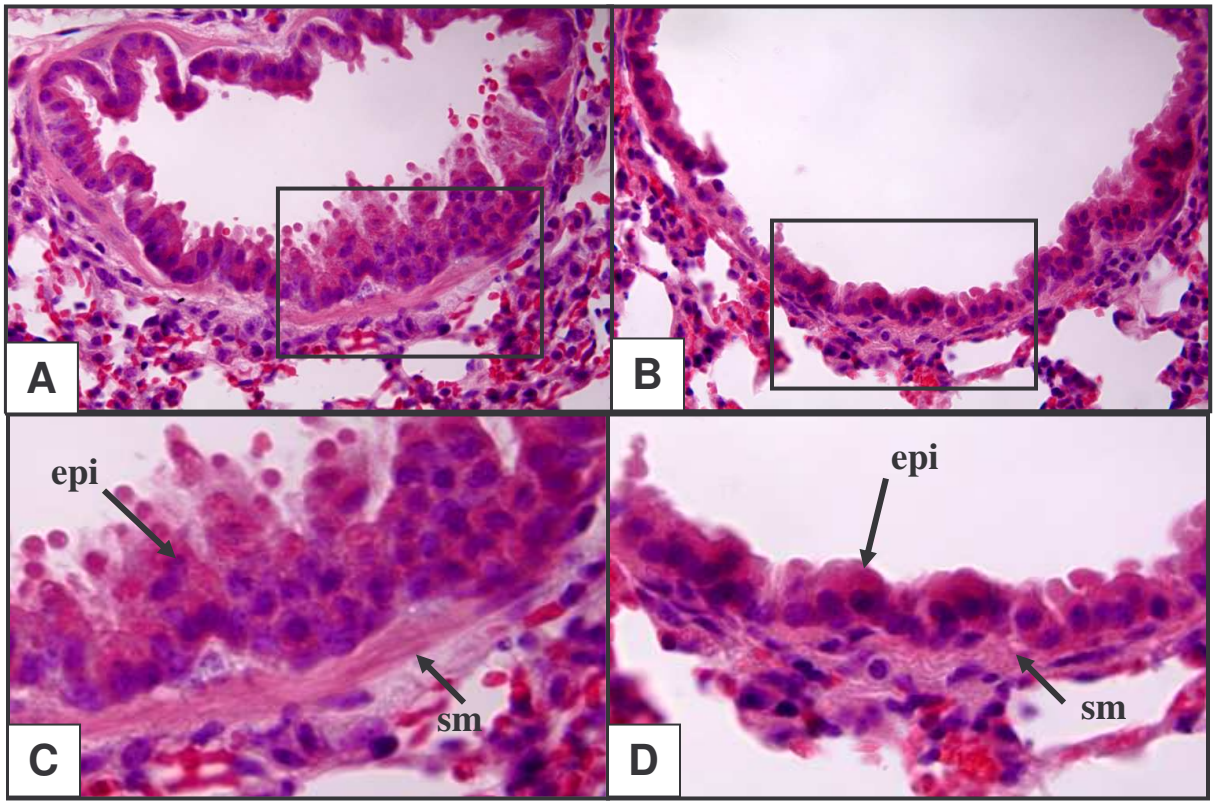

Figure 12: Hematoxylin and Eosin (H&E) staining of lung sections from a naïve caveolin-1 knockout animal (Cav-1 KO) **(A)(C)** and a naïve genetic control animal (B6129SF2/J) **(B)(D)**. Photographs were originally taken at 40x magnification. **A**: 6μm section from a Cav-1 KO mouse. **C**: enlarged view of area indicated in A showing thickened smooth muscle layer **(sm)** and thickened airway epithelium **(epi) B**: 6μm section from a B6129SF2J mouse showing a normal airway. **D**: Enlarged view of the area indicated in B.

Lung sections were also stained with Masson's Trichrome for a more detailed look at caveolin-1 knockout and B6129SF2/J lung structure. Masson's Trichrome stains nuclei black, collagen blue and cytoplasm, erythrocytes and muscle stains various shades of red. Again, considerable differences between airways from the knockout animals and control animals were observed (Figure 13). Airways from the caveolin-1 knockout mice had a folded epithelial layer and a thicker airway smooth muscle layer. There was also excessive blue staining surrounding the airways and associated blood vessels, indicating there may be excessive extracellular matrix surrounding these structures in the caveolin-1 knockout mice.

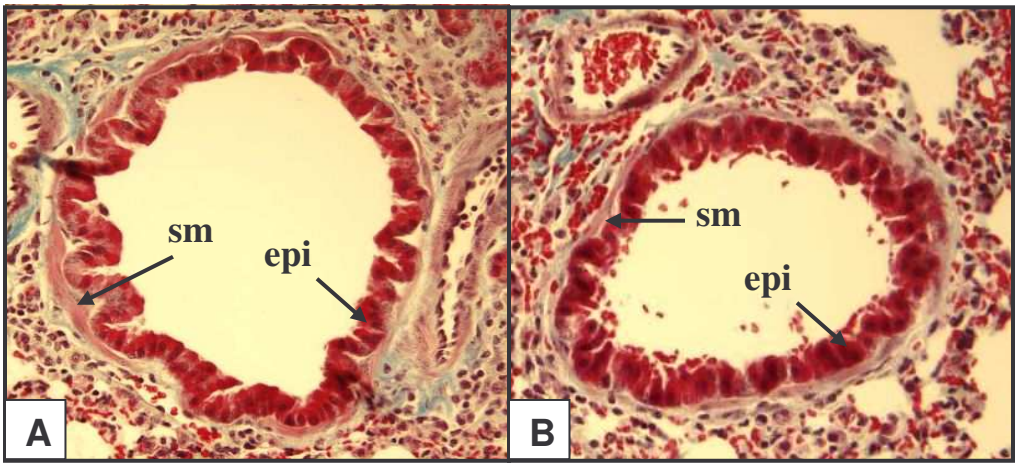

Figure 13: Masson's Trichrome staining of lung tissue sections from a naïve caveolin-1 knockout mouse (Cav-1 KO) **(A)** and a naïve genetic control animal (B6129SF2/J) **(B)**. Photographs were originally taken at 40x magnification. **A**: 6μm section from a Cav-1 KO mouse showing an airway with thickened airway smooth muscle layer **(sm)**(pink), folded airway epithelium**(epi)**(red) and excessive extracellular matrix (blue) surrounding airway and adjacent blood vessels. **B**: 6μm section from a B6129SF2/J mouse showing a normal airway.

Masson's Trichrome staining of the peripheral lung parenchyma from caveolin-1 knockout mice showed smaller alveolar spaces and hypercellular alveolar septa, resulting in thickened septal walls (Figure 14).

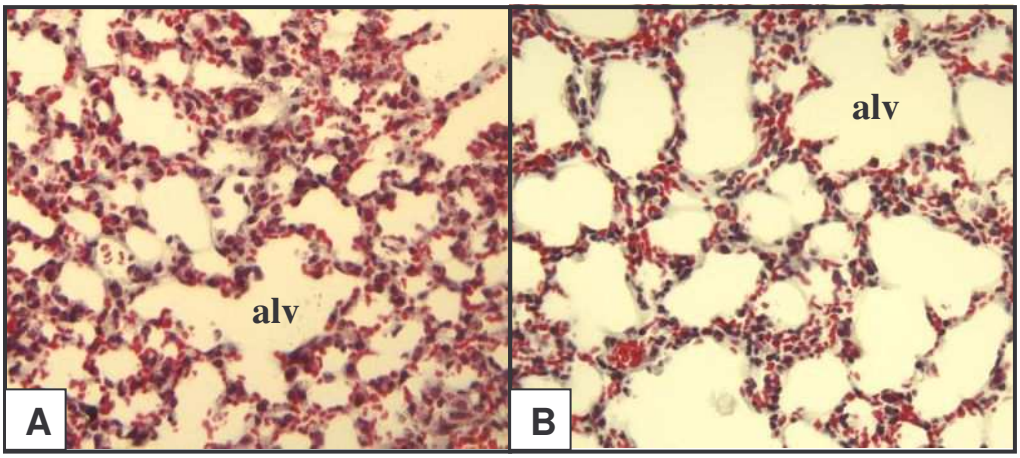

Figure 14: Masson's Trichrome staining of lung parenchyma from a naïve caveolin-1 knockout mouse (Cav-1 KO) **(A)** and a naive genetic control mouse (B6129SF2/J) **(B)**. Photographs were originally taken at 40x magnification. **A**: 6μm section from a Cav-1 KO mouse showing peripheral lung. Alveolar spaces **(alv)** are smaller and/or constricted and alveolar septa are thickened. **B**: 6μm section from a B6129SF2/J mouse showing a normal peripheral lung with large open alveolae.

4. Discussion

Allergen sensitization and challenge with ovalbumin induced a clinical syndrome which closely resembled allergic asthma in BALB/c mice. These mice demonstrated methacholine hyperresponsiveness and eosinophilic lung inflammation only after both sensitization by *i.p.* injection and intranasal challenge with ovalbumin. No differences in lung function were observed between the saline control group and OVA experimental group following sensitization, confirming that sensitization alone is insufficient to produce the airway hyperresponsiveness in mice that is typically associated with allergic asthma. Similarly, airway inflammation was not present following sensitization and only developed after intranasal exposure to ovalbumin. Therefore, the development of altered lung function appears to be dependent upon the inhalation of allergen, which triggers local airway inflammation. My studies show that the cellular inflammation induced by inhaled OVA in BALB/c mice is characterized by eosinophilia; a hallmark feature of asthma.

Unlike in BALB/c mice, our sensitization and challenge protocol did not induce methacholine hyperresponsiveness in either caveolin-1 knockout mice or the genetic control strain (B6129SF2/J). Shinagawa *et al.* (2003) demonstrated significant differences in mouse strain response to allergen sensitization and challenge. For example, A/J mice showed greater eosinophilic inflammation, airway hyperresponsiveness and histological changes compared to BALB/c, C57BL/6 and C3H/HeJ mice (Shinagawa *et al.,* 2003). In C57BL/6 mice, eosinophilic inflammation, airway hyperresponsiveness, and airway remodelling was not observed (Shinagawa *et al.,* 2003). This is consistent with other research which indicates strain differences may play a role in the development of airway hyperresponsiveness following allergen sensitization and challenge (Whitehead *et al.,* 2003). Since the caveolin-1 knockout and B6129SF2/J mice were developed on a C57BL/6 background, the immune response to our sensitization and challenge protocol may differ from BALB/c mice.

Our data revealed that eosinophilia was a feature of allergic inflammation in B6129SF2/J mice, although this inflammation did not result in airway hyperresponsiveness. This suggests this strain may differ in other fundamental features of inflammation that I did not measure, or in lung structure-function properties compared to BALB/c mice. For instance, it is possible that the initial sensitization requires a longer period of time compared to the BALB/c mice. If this is the case, the optimal time period between intraperitoneal injections for each strain studied needs to be determined. Some allergen sensitization and challenge protocols require up to 4 weeks between intraperitoneal injections to maximize the airway inflammation required for the development of airway hyperresponsiveness in mice (Epstein 2004). Since eosinophilia was muted in caveolin-1 knockout mice, it becomes particularly important to consider the temporal responses to sensitization in these mice. Unfortunately, our protocol does not allow me to determine if this differential inflammation is due to an overall suppressed response, or a difference in the kinetics of the airway inflammatory response. This suggests future experiments which study the temporal responses in cellular inflammation after allergen sensitization and challenge are warranted.

Unlike the BALB/c and B6129SF2/J mice, following sensitization and challenge, macrophages continued to be the major cell type found in caveolin-1 knockout BALF. Recent studies have shown that caveolin-1 is expressed by macrophages and may be involved in normal cell turnover and modulation of inflammatory responses (Gargalovic *et al.,* 2003; Wang *et al.,* 2005). For example, Gargalovic *et al.* (2003) demonstrated that apoptosis in macrophages is associated with an increase in caveolin-1 expression. Clearance of apoptotic cells from the body is mediated via the externalization of phosphotidylserine (PS). Externalization of PS acts as a signal to phagocytotic cells and the observed increase in caveolin-1 expression was found to be closely associated with this externalization (Gargalovic *et al.,* 2003). The specific role of caveolin-1 in these processes remains unclear; however, it is

possible that through its association with PS externalization, caveolin-1 may regulate macrophage apoptosis. If this is the case, the high percentage of macrophages seen in the caveolin-1 knockout BALF could be due to the lack of caveolin-1 mediated macrophage apoptosis.

Future studies will examine the actual cell counts to determine if the number of macrophages in the caveolin-1 knockout BALF increases, decreases, or remains the same after ovalbumin sensitization and challenge. Enzyme-linked immunosorbent assay (ELISA) will also be performed to get a more accurate inflammatory profile of these mice.

Penh values from the caveolin-1 knockout mice were approximately 50% lower at the higher doses of methacholine compared to B6129SF2/J mice. The difference between mouse strains was maintained prior to sensitization, following sensitization and following challenge, though this difference was only statistically significant at the higher doses of methacholine prior to and after sensitization. This indicates there is an intrinsic difference in the caveolin-1 knockout mice which makes them less responsive to bronchoconstrictive agents such as methacholine. Though the precise mechanism cannot be identified in my study, it is interesting to consider the possibility that the loss of caveolin-1 suppresses receptor mediated responses.

Airway response to inhaled bronchoconstrictive agents is controlled by cholinergic muscarinic receptor regulation of airway smooth muscle (Gosens *et al.,* 2004). In normal smooth muscle contraction, acetylcholine from parasympathetic cholinergic nerves binds to M3 receptors on the airway smooth muscle membrane. This binding eventually leads to muscle contraction via intracellular signaling events dependent on G protein coupled signaling, as well as sustained increases in intracellular calcium and smooth muscle myosin light chain activation (Borchers *et al.,* 2003). Borchers *et al.* (2003) demonstrated that mice deficient in Gαq are hyporesponsive to M3 receptor activation, indicating the importance of

Gαq for airway smooth muscle contraction. Interestingly, the loss of caveolin-1 has been linked to the disruption of M3 associated signaling in the smooth muscle of the urinary bladder (Lai *et al.,* 2004). Similarly, the loss of caveolin-1 may also disrupt M3 receptor signaling in the lung and thus impair airway smooth muscle contraction, which is consistent with the hyporesponsiveness observed in the knockout mice. This signal disruption may be due to the alteration of G protein coupled downstream signaling or an inability to activate the M3 receptor when caveolae are absent. Further studies will need to be completed to identify which signaling molecules are affected with ablation of caveolae.

Borchers *et al.* (2003) determined that Gαq deficient mice failed to develop an increase in airway responsiveness to methacholine following ovalbumin sensitization and challenge. Our caveolin-1 knockout mice also failed to develop airway hyperresponsiveness after ovalbumin sensitization and challenge, indicating that G protein coupled signaling may be affected with the loss of caveolae. Since many G protein coupled receptors, such as endothelin, and the M3 muscarinic receptor are associated with and sometimes localized in caveolae, the loss of these structures in the plasma membrane may result in the disruption of the associated signal transduction pathways (Bergdahl *et al.,* 2004; Chun *et al.,* 1994). The failure of caveolin-1 knockout mice to become hyperresponsive to methacholine after allergen challenge correlates well with the blunted eosinophilic inflammation I measured. This suggests that both reduced eosinophilia and changes in muscarinic receptor mediated signaling in caveolin-1 knockout mice could contribute to lung hyporesponsiveness.

Caveolin-1 knockout mice showed significant differences in lung structure, similar to airway remodelling, compared to B6129SF2/J mice. Hematoxylin and Eosin staining, as well as Masson's Trichrome staining, revealed a more prominent smooth muscle layer, thickened epithelium, and increased extracellular matrix surrounding the airways and associated blood vessels in caveolin-1 knockout animals. Surprisingly, these differences were observed prior to

allergen sensitization and challenge; whereas, the structural changes associated with airway remodelling results from repeated and prolonged exposure to allergens. Our data suggests that functionally important pre-existing remodelling exists in caveolin-1 knockout mice. The paradox that emerges is that the remodelling observed in caveolin-1 knockout mice suppressed airway responses. Clearly, future work in which more invasive measurement of respiratory mechanics will be needed to decipher the structure-function relationship that exists in caveolin-1 knockout animals.

Airway smooth muscle has two phenotypes, contractile and synthetic (Halayko *et al.,* 2001; Halayko *et al.,* 2003). Serum and growth factors can induce a switch in airway smooth muscle phenotype associated with decreased contractility and increased proliferation through interaction with the p42/p44 mitogen activated protein kinase pathway (MAPK) (Gosens *et al.,* 2004). This pathway is involved in promoting muscle cell proliferation (Gosens *et al.,* 2004). Gosens *et al.* (2006) demonstrated, with the use of silencing RNA, that the removal of caveolin-1 results in an increase in basal p42/p44 MAPK activation, and excessive proliferation. This indicates that caveolin-1 normally functions to inhibit cell proliferation, and thus may explain why airway smooth muscle mass was significantly greater in caveolin-1 knockout mice. Surprisingly, despite the fact that they exhibited excessive airway smooth muscle, the caveolin-1 knockout mice were hyporesponsive to methacholine during lung function tests. This suggests the airway smooth muscle is proliferating, possibly due to the upregulation of the p42/p44 MAPK pathway, and not contracting. Further studies will be performed using isolated bronchial rings and a multi-chamber myograph to fully characterize the phenotype of the airway smooth muscle in caveolin-1 knockout mice.

The proliferative phenotype of smooth muscle is also associated with increased synthetic function of the cells (Halayko *et al.,* 2001). We observed that caveolin-1 knockout animals showed excessive amounts of fibrosis in the airways, suggesting the lack of caveolin-1

contributes to airway fibrosis, due to effects of smooth muscle phenotype. This is consistent with emerging data which reveals caveolin-1 inhibits the signal transduction of pro-fibrotic pathways (Razani *et al.,* 2001b; Williams *et al.,* 2004). Thus the loss of this inhibition, due to the loss of caveolin-1, may lead to extracellular matrix synthesis induced by asthma-associated pro-inflammatory molecules such as transforming growth factor β (TGF-β) (Razani *et al.,* 2001b; Schwartz *et al.,* 2005). Interestingly, caveolin-1 knockout mice also show reductions in life span due to pulmonary fibrosis, further strengthening the idea that the removal of caveolin-1 leads to extracellular matrix synthesis (Park *et al.,* 2003).

The alveolar spaces were smaller or constricted in caveolin-1 knockout mice and the alveolar septa were thickened. These findings are similar to those described by Razani and Lisanti (2001) in their characterization of caveolin-1 knockout mice. Other studies have shown marked hypercellularity in the lungs of these mice due to significant increases in endothelial cell number (Drab *et al.,* 2001; Razani *et al.,* 2001a; Razani *et al.,* 2001c). Staining with Ki67 also revealed that cellular proliferation was markedly increased in caveolin-1 null lungs (Razani *et al.,* 2001a; Razani *et al.,* 2001c). This hypercellularity and increased cellular proliferation stresses the importance of caveolin-1 as a regulator of proliferation.

4.1 Conclusion

The expression of caveolin-1 appears to be a significant determinant of lung structure and function. When caveolin-1 expression is knocked out, the plasma membrane invaginations associated with many signal transduction pathways are lost. The loss of caveolin-1 and caveolae in the lung results in increased proliferation of airway smooth muscle and endothelial cells, as well as increased deposition of extracellular matrix around airways and blood vessels. Also, the alveolar spaces are reduced and septa are thickened. Surprisingly, the extra smooth muscle does not appear functional as caveolin-1 knockout mice are hyporesponsive to methacholine during lung function tests. Finally, caveolin-1 knockout mice exhibit a differential inflammatory response in comparison to the increased eosinophilia

observed in BALB/c and B6129SF2/J mice following ovalbumin sensitization and challenge. Collectively, these data suggest that caveolin-1 may modulate airway function and orchestrate local inflammation. Thus, further studies to dissect the role of this protein in asthma pathogenesis are warranted.

5. References

Adler A, Cieslewicz G, Irvin CG. 2004. Unrestrained plethysmography is an unreliable measure of airway responsiveness in BALB/c and C57BL/6 mice. Journal of Applied Physiology: Respiratory, Environmental and Exercise Physiology 97(1):286-292.

Alkan SS, Akdis AC, Feuerlein D, Gruninger M. 1996. Direct measurement of cytokines (IFN-gamma, IL-4, -5, and -6) from organs after antigenic challenge. Annals of the New York Academy of Sciences 796:82-90.

Bai TR and Knight DA. 2005. Structural changes in the airways in asthma: observations and consequences. Clinical Science 108(6):463-477.

Bergdahl A and Sward K. 2004. Caveolae-associated signalling in smooth muscle. Canadian Journal of Physiology and Pharmacology 82(5):289-299.

Borchers MT, Biechele T, Justice JP, Ansay T, Cormier S, Mancino V, Wilkie TM, Simon MI, Lee NA, Lee JJ. 2003. Methacholine-induced airway hyperresponsiveness is dependent on Galphaq signaling. American Journal of Physiology. Lung Cellular and Molecular Physiology 285(1):L114-L120.

Boulet L, Becker A, Bowie D, McIvor A, Hernandez P, Rouleau M, Bourbeau J, Graham I, Legare F, Ward T, and others. 2006. Implementing practice guidelines: A workshop on guidelines dissemination and implementation with a focus on asthma and COPD. Canadian Respiratory Journal : Journal of the Canadian Thoracic Society 13 Suppl A:5-47.

Bucci M, Gratton JP, Rudic RD, Acevedo L, Roviezzo F, Cirino G, Sessa WC. 2000. In vivo delivery of the caveolin-1 scaffolding domain inhibits nitric oxide synthesis and reduces inflammation. Nature Medicine 6(12):1362-1367.

Cates EC, Gajewska BU, Goncharova S, Alvarez D, Fattouh R, Coyle AJ, Gutierrez-Ramos JC, Jordana M. 2003. Effect of GM-CSF on immune, inflammatory, and clinical responses to ragweed in a novel mouse model of mucosal sensitization. The Journal of Allergy and Clinical Immunology 111(5):1076-1086.

Chun M, Liyanage UK, Lisanti MP, Lodish HF. 1994. Signal transduction of a G protein-coupled receptor in caveolae: colocalization of endothelin and its receptor with caveolin. Proceedings of the National Academy of Sciences of the United States of America 91(24):11728-11732.

Cockcroft DW. 1985. Bronchial inhalation tests. I. Measurement of nonallergic bronchial responsiveness. Annals of Allergy 55(4):527-534.

Drab M, Verkade P, Elger M, Kasper M, Lohn M, Lauterbach B, Menne J, Lindschau C, Mende F, Luft FC, and others. 2001. Loss of caveolae, vascular dysfunction, and pulmonary defects in caveolin-1 gene-disrupted mice. Science 293(5539):2449-2452.

Dreja K, Voldstedlund M, Vinten J, Tranum-Jensen J, Hellstrand P, Sward K. 2002. Cholesterol depletion disrupts caveolae and differentially impairs agonist-induced arterial contraction. Arteriosclerosis, Thrombosis, and Vascular Biology 22(8):1267-1272.

Epstein MM. 2004. Do mouse models of allergic asthma mimic clinical disease? International Archives of Allergy and Immunology 133(1):84-100.

Eum SY, Maghni K, Tolloczko B, Eidelman DH, Martin JG. 2005. IL-13 may mediate allergen-induced hyperresponsiveness independently of IL-5 or eotaxin by effects on airway smooth muscle. American Journal of Physiology. Lung Cellular and Molecular Physiology 288(3):L576-84.

Galbiati F, Razani B, Lisanti MP. 2001. Emerging themes in lipid rafts and caveolae. Cell 106(4):403-411.

Garcia-Cardena G, Oh P, Liu J, Schnitzer JE, Sessa WC. 1996. Targeting of nitric oxide synthase to endothelial cell caveolae via palmitoylation: implications for nitric oxide signaling. Proceedings of the National Academy of Sciences of the United States of America 93(13):6448-6453.

Gargalovic P and Dory L. 2003. Cellular apoptosis is associated with increased caveolin-1 expression in macrophages. Journal of Lipid Research 44(9):1622-1632.

Ghosh S, Gachhui R, Crooks C, Wu C, Lisanti MP, Stuehr DJ. 1998. Interaction between caveolin-1 and the reductase domain of endothelial nitric-oxide synthase. Consequences for catalysis. Journal of Biological Chemistry 273(35):22267-22271.

Gosens R, Stelmack, GL, Dueck G, McNeill KD, Yamasaki A, Gerthoffer WT, Unruh H, Zaagsma J, Halayko A. 2006. Role of caveolin-1 in p42/p44 MAP kinase activation and proliferation of human airway smooth muscle. In Press. American Journal of Physiology.

Gosens R, Bromhaar MM, Tonkes A, Schaafsma D, Zaagsma J, Nelemans SA, Meurs H. 2004. Muscarinic M(3) receptor-dependent regulation of airway smooth muscle contractile phenotype. British Journal of Pharmacology 141(6):943-950.

Halayko AJ and Stelmack GL. 2005. The association of caveolae, actin, and the dystrophin-glycoprotein complex: a role in smooth muscle phenotype and function? Canadian Journal of Physiology and Pharmacology 83(10):877-891.

Halayko AJ and Amrani Y. 2003. Mechanisms of inflammation-mediated airway smooth muscle plasticity and airways remodeling in asthma. Respiratory Physiology & Neurobiology 137(2-3):209-222.

Halayko AJ and Solway J. 2001. Molecular mechanisms of phenotypic plasticity in smooth muscle cells. Journal of Applied Physiology: Respiratory, Environmental and Exercise Physiology 90(1):358-368.

Hamelmann E, Schwarze J, Takeda K, Oshiba A, Larsen GL, Irvin CG, Gelfand EW. 1997. Noninvasive measurement of airway responsiveness in allergic mice using barometric plethysmography. American Journal of Respiratory and Critical Care Medicine : An

Official Journal of the American Thoracic Society, Medical Section of the American Lung Association 156(3 Pt 1):766-775.

Hayashi K, Matsuda S, Machida K, Yamamoto T, Fukuda Y, Nimura Y, Hayakawa T, Hamaguchi M. 2001. Invasion activating caveolin-1 mutation in human scirrhous breast cancers. Cancer Research 61(6):2361-2364.

Henderson WR,Jr, Tang LO, Chu SJ, Tsao SM, Chiang GK, Jones F, Jonas M, Pae C, Wang H, Chi EY. 2002. A role for cysteinyl leukotrienes in airway remodeling in a mouse asthma model. American Journal of Respiratory and Critical Care Medicine : An Official Journal of the American Thoracic Society, Medical Section of the American Lung Association 165(1):108-116.

Hnasko R and Lisanti MP. 2003. The biology of caveolae: lessons from caveolin knockout mice and implications for human disease. Molecular Interventions 3(8):445-464.

Justice JP, Borchers MT, Lee JJ, Rowan WH, Shibata Y, Van Scott MR. 2002. Ragweed-induced expression of GATA-3, IL-4, and IL-5 by eosinophils in the lungs of allergic C57BL/6J mice. American Journal of Physiology. Lung Cellular and Molecular Physiology 282(2):L302-9.

Khan AM, Elidemir O, Epstein CE, Lally KP, Xue H, Blackburn M, Larsen GL, Colasurdo GN. 2002. Meconium aspiration produces airway hyperresponsiveness and eosinophilic inflammation in a murine model. American Journal of Physiology. Lung Cellular and Molecular Physiology 283(4):L785-90.

Kim J, Merry AC, Nemzek JA, Bolgos GL, Siddiqui J, Remick DG. 2001. Eotaxin represents the principal eosinophil chemoattractant in a novel murine asthma model induced by house dust containing cockroach allergens. Journal of Immunology 167(5):2808-2815.

Lai HH, Boone TB, Yang G, Smith CP, Kiss S, Thompson TC, Somogyi GT. 2004. Loss of caveolin-1 expression is associated with disruption of muscarinic cholinergic activities in the urinary bladder. Neurochemistry International 45(8):1185-1193.

Leigh R, Ellis R, Wattie J, Southam DS, De Hoogh M, Gauldie J, O'Byrne PM, Inman MD. 2002. Dysfunction and remodeling of the mouse airway persist after resolution of acute allergen-induced airway inflammation. American Journal of Respiratory Cell and Molecular Biology : An Official Journal of the American Thoracic Society, Medical Section of the American Lung Association 27(5):526-535.

Li XA, Everson WV, Smart EJ. 2005. Caveolae, lipid rafts, and vascular disease. Trends in Cardiovascular Medicine 15(3):92-96.

Macleod KF and Jacks T. 1999. Insights into cancer from transgenic mouse models. The Journal of Pathology 187(1):43-60.

Michel JB, Feron O, Sacks D, Michel T. 1997a. Reciprocal regulation of endothelial nitric-oxide synthase by Ca2+-calmodulin and caveolin. Journal of Biological Chemistry 272(25):15583-15586.

Michel JB, Feron O, Sase K, Prabhakar P, Michel T. 1997b. Caveolin versus calmodulin. Counterbalancing allosteric modulators of endothelial nitric oxide synthase. Journal of Biological Chemistry 272(41):25907-25912.

Mojtabavi N, Dekan G, Stingl G, Epstein MM. 2002. Long-lived Th2 memory in experimental allergic asthma. Journal of Immunology 169(9):4788-4796.

Murata M, Peranen J, Schreiner R, Wieland F, Kurzchalia TV, Simons K. 1995. VIP21/caveolin is a cholesterol-binding protein. Proceedings of the National Academy of Sciences of the United States of America 92(22):10339-10343.

O'Brien R, Ooi MA, Clarke AH, Thomas WR. 1996. Immunologic responses following respiratory sensitization to house dust mite allergens in mice. Immunology and Cell Biology 74(2):174-179.

Park DS, Cohen AW, Frank PG, Razani B, Lee H, Williams TM, Chandra M, Shirani J, De Souza AP, Tang B, and others. 2003. Caveolin-1 null (-/-) mice show dramatic reductions in life span. Biochemistry (John Wiley & Sons) 42(51):15124-15131.

Racine C, Belanger M, Hirabayashi H, Boucher M, Chakir J, Couet J. 1999. Reduction of Caveolin 1 Gene Expression in Lung Carcinoma Cell Lines. Biochemical and Biophysical Research Communications 255(3):580-586.

Razani B and Lisanti MP. 2001a. Caveolin-deficient mice: insights into caveolar function human disease. The Journal of Clinical Investigation 108(11):1553-1561.

Razani B, Zhang XL, Bitzer M, von Gersdorff G, Bottinger EP, Lisanti MP. 2001b. Caveolin-1 regulates transforming growth factor (TGF)-beta/SMAD signaling through an interaction with the TGF-beta type I receptor. Journal of Biological Chemistry 276(9):6727-6738.

Razani B, Engelman JA, Wang XB, Schubert W, Zhang XL, Marks CB, Macaluso F, Russell RG, Li M, Pestell RG, and others. 2001c. Caveolin-1 null mice are viable but show evidence of hyperproliferative and vascular abnormalities. Journal of Biological Chemistry 276(41):38121-38138.

Redington AE. 2000. Fibrosis and airway remodelling. Clinical and experimental allergy : Journal of the British Society for Allergy and Clinical Immunology 30 Suppl 1:42-45.

Schubert W, Frank PG, Razani B, Park DS, Chow CW, Lisanti MP. 2001. Caveolae-deficient endothelial cells show defects in the uptake and transport of albumin in vivo. Journal of Biological Chemistry 276(52):48619-48622.

Schwartz EA, Reaven E, Topper JN, Tsao PS. 2005. Transforming growth factor-beta receptors localize to caveolae and regulate endothelial nitric oxide synthase in normal human endothelial cells. The Biochemical Journal 390(Pt 1):199-206.

Shinagawa K and Kojima M. 2003. Mouse model of airway remodeling: strain differences. American Journal of Respiratory and Critical Care Medicine : An Official Journal of the

American Thoracic Society, Medical Section of the American Lung Association 168(8):959-967.

Simons K and Ikonen E. 1997. Functional rafts in cell membranes. Nature 387(6633):569-572.

Smart EJ, Graf GA, McNiven MA, Sessa WC, Engelman JA, Scherer PE, Okamoto T, Lisanti MP. 1999. Caveolins, liquid-ordered domains, and signal transduction. Molecular and Cellular Biology 19(11):7289-7304.

The National Asthma Control Task Force. 2000. The Prevention and management of asthma in Canada: a major challenge now and in the future.

Wagers S, Lundblad LK, Ekman M, Irvin CG, Bates JH. 2004. The allergic mouse model of asthma: normal smooth muscle in an abnormal lung? Journal of Applied Physiology: Respiratory, Environmental and Exercise Physiology 96(6):2019-2027.

Wang XM, Kim HP, Song R, Choi AM. 2005. Caveolin-1 Confers Anti-Inflammatory Effects in Murine Macrophages via the MKK3/p38 MAPK Pathway. American Journal of Respiratory Cell and Molecular Biology : An Official Journal of the American Thoracic Society, Medical Section of the American Lung Association 34(): 434-442.

Whitehead GS, Walker JK, Berman KG, Foster WM, Schwartz DA. 2003. Allergen-induced airway disease is mouse strain dependent. American Journal of Physiology. Lung Cellular and Molecular Physiology 285(1):L32-L42.

Williams TM and Lisanti MP. 2004. The Caveolin genes: from cell biology to medicine. Annals of Medicine 36(8):584-595.

Yamada E. 1955. The fine structure of the gall bladder epithelium of the mouse. Journal of Biophysiology, Biochemistry & Cytology 1(5):445-458.

Yang X, Wang S, Fan Y, Zhu L. 1999. Systemic mycobacterial infection inhibits antigen-specific immunoglobulin E production, bronchial mucus production and eosinophilic inflammation induced by allergen. Immunology 98(3):329-337.

Yu CK, Shieh CM, Lei HY. 1999. Repeated intratracheal inoculation of house dust mite (Dermatophagoides farinae) induces pulmonary eosinophilic inflammation and IgE antibody production in mice. The Journal of Allergy and Clinical Immunology 104(1):228-236.

6. Appendix

6.1 Recipes

6.1.1 Methacholine (MCh) Preparation

Methacholine solutions (Sigma; catalogue # A2251-100G) were prepared for lung function tests by serial dilution to obtain concentrations ranging from 3.1 mg/ml to 50mg/ml (Figure 15).

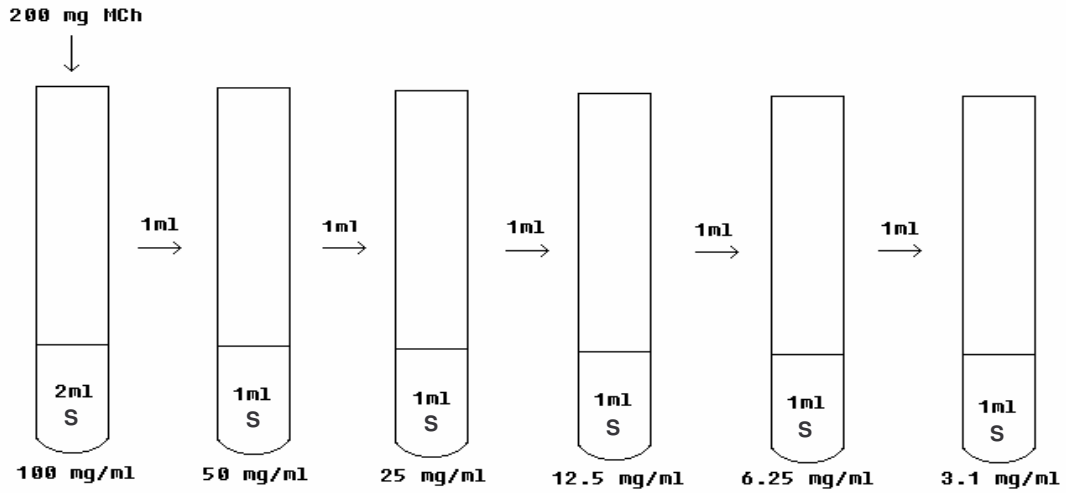

Figure 15: Preparation of methacholine solutions by serial dilution. S= saline.

6.1.2 Wiegert's Iron Hematoxylin

Wiegert's Iron Hematoxylin was prepared for Trichrome staining by mixing equal volumes of Part A and Part B from the Wiegert's Iron Hematoxylin Set (Sigma Aldrich; catalogue # HT1079-1SET).

6.1.3. Phosphotungstic/Phosphomolybdic acid solution

Phosphotungstic/phosphomolybdic acid solution was prepared for Masson's Trichrome staining by mixing 1 volume of phosphotungstic acid with 1 volume of phosphomolybdic acid and 2 volumes of distilled water. Solutions were provided with the Masson's Trichrome staining kit (Sigma Aldrich; catalogue # HT15-1KT).